

NOTE TO USERS

This reproduction is the best copy available.

UMI[®]

**THE SOLUBILITY AND SPECIATION OF MOLYBDENUM IN WATER
VAPOUR AT ELEVATED TEMPERATURES AND PRESSURES:
IMPLICATIONS FOR ORE GENESIS**

Kirsten U. Rempel

October, 2004

A thesis submitted to McGill University in partial fulfillment of the requirements of
the degree of Master of Science

Department of Earth and Planetary Science
McGill University
Montreal, Quebec
Canada

© Kirsten U. Rempel, 2004



Library and
Archives Canada

Bibliothèque et
Archives Canada

Published Heritage
Branch

Direction du
Patrimoine de l'édition

395 Wellington Street
Ottawa ON K1A 0N4
Canada

395, rue Wellington
Ottawa ON K1A 0N4
Canada

Your file *Votre référence*

ISBN: 0-494-12526-8

Our file *Notre référence*

ISBN: 0-494-12526-8

NOTICE:

The author has granted a non-exclusive license allowing Library and Archives Canada to reproduce, publish, archive, preserve, conserve, communicate to the public by telecommunication or on the Internet, loan, distribute and sell theses worldwide, for commercial or non-commercial purposes, in microform, paper, electronic and/or any other formats.

The author retains copyright ownership and moral rights in this thesis. Neither the thesis nor substantial extracts from it may be printed or otherwise reproduced without the author's permission.

AVIS:

L'auteur a accordé une licence non exclusive permettant à la Bibliothèque et Archives Canada de reproduire, publier, archiver, sauvegarder, conserver, transmettre au public par télécommunication ou par l'Internet, prêter, distribuer et vendre des thèses partout dans le monde, à des fins commerciales ou autres, sur support microforme, papier, électronique et/ou autres formats.

L'auteur conserve la propriété du droit d'auteur et des droits moraux qui protègent cette thèse. Ni la thèse ni des extraits substantiels de celle-ci ne doivent être imprimés ou autrement reproduits sans son autorisation.

In compliance with the Canadian Privacy Act some supporting forms may have been removed from this thesis.

Conformément à la loi canadienne sur la protection de la vie privée, quelques formulaires secondaires ont été enlevés de cette thèse.

While these forms may be included in the document page count, their removal does not represent any loss of content from the thesis.

Bien que ces formulaires aient inclus dans la pagination, il n'y aura aucun contenu manquant.


Canada

Abstract

The solubility of molybdenum trioxide in liquid-undersaturated water vapour has been investigated experimentally at 300, 320, and 360°C and 48 to 163 bars. Results of these experiments show that the solubility of MoO_3 in the vapour phase is between 1 and 23 ppm, which is 19-20 orders of magnitude higher than that in a water-free system. Molybdenum solubilities increase linearly with f_{H_2O} , indicating that the metal forms a gaseous hydrated complex of the type $MoO_3 \cdot nH_2O$ by the reaction:



The hydration number, n , is interpreted to have a value of 2.6 at 300°C, 2.5 at 320°C, and 3.0 at 360°C. Values of $\log K$ for this reaction are 16.9 at 300°C, 16.5 at 320°C, and 12.5 at 360°C.

Calculations based on the extrapolated solubility of MoO_3 in equilibrium with molybdenite at 600°C and 500 bars, using average H_2O and total S fluxes of actively degassing volcanoes, with f_{O_2} and f_{S_2} controlled by the assemblage hematite-magnetite-pyrite, indicate that the vapour phase can transport sufficient Mo in about 900,000 years (within the life of some geothermal systems) to form a deposit of 336 Mt, with an average grade of 0.087% Mo (e.g., the Endako Mo -porphyry deposit, Canada).

Résumé

La solubilité du trioxyde de molybdène en phase gazeuse sous-saturée en liquide a été étudiée expérimentalement à des températures de 300, 320 et 360°C et à des pressions variant de 48 à 178 bars. Les résultats de ces expériences indiquent que la solubilité du MoO_3 dans la phase vapeur varie entre 1 et 35 ppm, ce qui est de 19 à 20 ordres de grandeur plus élevé que dans un système anhydre. La solubilité du MoO_3 augmente de façon linéaire avec l'accroissement de la fugacité de l'eau. Ceci indique que le trioxyde de molybdène forme une phase gazeuse hydratée du type $MoO_3 \cdot nH_2O$ via la réaction:



Le degré d'hydratation (n) varie de 2,6 à 300°C à 2,1 à 320°C et 2,9 à 360°C. Le logarithme de la constante d'équilibre ($\log K$) est, respectivement, de 16,9, 16,5 et 12,5.

En extrapolant la solubilité du MoO_3 en équilibre avec la molybdénite à 600°C et 500 bars, en utilisant le flux moyen de H_2O et de S du dégazage volcanique, et avec des fugacités de O_2 et S_2 contrôlées par le tampon hématite-magnétite-pyrite, nous démontrons que la phase vapeur peut transporter assez de molybdène en 900,000 ans (durée de vie de plusieurs systèmes géothermales) pour qu'un gîte de type porphyrique de 336 Mt à 0,087% Mo (i.e., le porphyre à Mo d'Endako, Colombie-Britannique) puisse se former.

Acknowledgements

Many thanks to Dr. A.E. Williams-Jones, for his innovative ideas and enthusiasm for research, and without whom this thesis would never have been started. Also thanks to Dr. A.A. Migdisov, whose patient guidance calmed many a panic attack, and who has turned the hieroglyphics of thermodynamics into something a little more comprehensible.

I would also like to thank J.R. Clark, Dr. S.A. Archibald, Dr. J. Stix, and V. Reukov for helpful input and insightful discussions of my research. For technical help and analytical work, thanks go to D. Reid, T. Ahmedali, G. Keating, and B. Dionne. I would also like to thank S. Kecani, for getting those autoclaves made, no matter how many tools got broken. Thanks also to Dr. S.M. Rowins, who is always ready with a letter of reference, and who helped me on my way.

Thanks to all of those who have made the department a good working environment, including J. Hartzler, K. Ault, O. Nadeau, A. Harlap, M. Mlynarczyk, and many others. Sincerest gratitude to A. Kosowski, who has an answer for every question. And finally, thanks to K. McCann, for getting me through that first year.

This project was funded in part by NSERC and FCAR grants awarded to A.E. Williams-Jones, and by departmental Lynch and LeRoy fellowships and a GEOTOP bursary awarded to the author.

Table of Contents

Abstract.....	i
Résumé.....	ii
Acknowledgements.....	iii
Table of contents.....	iv
List of figures.....	vi
List of tables.....	vii
Preface: Contributions of authors.....	viii
Chapter 1: General introduction.....	1
1.1. The vapour transport of metals.....	2
1.2. Thermodynamic estimates of metal volatility.....	3
1.3. Evidence of vapour transport from natural settings.....	4
1.3.1. Fluid inclusion evidence.....	4
1.3.2. Fumarolic condensates and sublimates.....	5
1.4. Experimental data in support of vapour transport of metals.....	8
1.5. Molybdenum speciation in aqueous liquids.....	9
1.5.1. Pearson's HSAB principle.....	9
1.5.2. Molybdenum speciation in hydrothermal liquids.....	10
1.5.3. Molybdenum hydrate stability in aqueous and acidic liquids...	12
1.6. Gaseous molybdenum speciation.....	13
1.6.1. Molybdenum volatility in dry systems.....	13
1.6.2. Thermodynamic modeling.....	15
1.6.3. Partitioning of <i>Mo</i> between magmas and aqueous fluid.....	17

1.6.4. Experimental data in support of the vapour transport of Mo....	18
1.7. Objectives of the study.....	20
1.8. Thesis organization.....	21
1.9. References.....	23
Introduction to Chapter 2.....	30
Chapter 2: The solubility and speciation of molybdenum in water vapour at elevated temperatures and pressures: implications for ore genesis.....	31
2.1. Abstract.....	32
2.2. Introduction.....	33
2.3. Experimental method.....	34
2.4. Results.....	37
2.5. Discussion.....	44
2.5.1. Data treatment.....	44
2.5.2. Oxidation state of molybdenum.....	47
2.5.3. Stability of hydrated species.....	48
2.5.4. Comparison with other studies.....	51
2.5.5. Geological implications.....	56
2.6. Conclusions.....	57
2.7. References.....	59
Chapter 3: Extended conclusions.....	64
Conclusions.....	65
Recommendations for future work.....	66
References.....	68
Appendix: Extrapolation of experimental data to high temperatures.....	69
References.....	72

List of figures

Figure 2-1: Schematic diagram of the titanium autoclaves employed in the experiments.....	36
Figure 2-2: Results of kinetic runs at 320°C, showing the change in molybdenum concentration ($\log f_{\text{MoO}_3 \cdot n\text{H}_2\text{O}}$) with time.....	38
Figure 2-3: A plot of $\log f_{\text{MoO}_3 \cdot n\text{H}_2\text{O}}$ versus $\log f_{\text{H}_2\text{O}}$ for 300°C, 320°C, and 360°C.....	39
Figure 2-4: A plot of $\log f_{\text{MoO}_3 \cdot n\text{H}_2\text{O}}$ versus $\log f_{\text{H}_2\text{O}}$ for dry and wet systems at 320°C.....	45
Figure 2-5: A plot of $\log f_{\text{MoO}_3 \cdot n\text{H}_2\text{O}}$ versus $\log f_{\text{H}_2\text{O}}$ for buffered and non-buffered experiments at 320°C.....	49
Figure 2-6: A plot of $\log f_{\text{Mo}}$ versus $\log f_{\text{H}_2\text{O}}$ at 1200-1500 °C, from Belton and Jordan (1963).....	52
Figure 2-7: A plot of hydration number (n) versus reciprocal temperature.....	54
Figure 2-8: A plot of the logarithm of the equilibrium constant for the reaction $\text{MoO}_3(g) + n\text{H}_2\text{O}(g) = \text{MoO}_3 \cdot n\text{H}_2\text{O}(g)$ versus reciprocal temperature.....	55

List of tables

Table 2-1: Results of experiments measuring the solubility of <i>Mo</i> in water vapour at 300°C.....	41
Table 2-2: Results of experiments measuring the solubility of <i>Mo</i> in water vapour at 320°C.....	42
Table 2-3: Results of experiments measuring the solubility of <i>Mo</i> in water vapour at 360°C.....	43

Preface: Contributions of authors

The research presented in this thesis is a result of collaboration between the author, Dr. A.E. Williams-Jones and Dr. A.A. Migdisov. The thesis is comprised of three chapters: a general introduction, a manuscript which has been submitted to *Geochimica et Cosmochimica Acta*, and an extended conclusion. Dr. A.A. Migdisov, the second author of the manuscript, provided guidance with the experimental method and data interpretation. The third author of the paper, Dr. A.E. Williams-Jones, acted as thesis supervisor, providing general research guidance and assistance with data evaluation, and doing critical reviews of the text. ICP-MS analyses of molybdenum concentrations were performed Dr. D. Reid of Activation Laboratories, Ancaster, Ontario. Training in XRD analysis was provided by T. Ahmedali and G. Keating, although the author performed all XRD analyses herself. All experimental work, data analysis, and writing was done by the author.

The following is an excerpt from the *Guidelines for Thesis Preparation* from the Faculty of Graduate and Postdoctoral Studies at McGill University:

“Candidates have the option of including as part of the thesis the text of one or more papers submitted, or to be submitted, for publication, or the clearly-duplicated text...of one or more published papers. These texts must...be bound together as an integral part of the thesis...”

“The thesis must be more than a collection of manuscripts. All components must be integrated into a cohesive unit with a logical progression from one chapter to the next. In order to ensure that the thesis has continuity, connecting texts that provide logical bridges preceding and following each manuscript are mandatory.

“...The thesis must contain the following: a table of contents; a brief abstract in both English and French; an introduction that clearly states the rationale and objectives of the research; a comprehensive review of the literature...a final conclusion and summary; a thorough bibliography...

“As manuscripts for publication are frequently very concise documents, where appropriate, additional material must be provided (e.g., in appendices) in sufficient detail to allow a clear and precise judgment to be made of the importance and originality of the research reported in the thesis.

“In general, when co-authored papers are included in a thesis the candidate must have made a substantial contribution to all papers included in the thesis. In addition, the candidate is required to make an explicit statement in the thesis as to who contributed to such work and to what extent. This statement should appear in a single section entitled “Contributions of Authors” as a preface to the thesis...Since the task of the examiners is made more difficult in these cases it is in the candidate’s interest to clearly specify the responsibilities of all the authors of the co-authored papers.”

CHAPTER 1

GENERAL INTRODUCTION

1.1. The vapour transport of metals

Conventional models for the formation of hydrothermal mineral deposits have considered an aqueous liquid to be the dominant agent for ore metal transport (e.g., reviews by White *et al.*, 1981; Wood and Samson, 1998). Until recently, the possibility of metal transport by an aqueous vapour has been largely ignored, due in part to early thermodynamic calculations which suggested that the solubility of metals in aqueous vapour was negligible (e.g., Krauskopf 1957, 1964). These calculations, however, failed to take into account possible interactions of the metals with the vapour that might enhance solvation. Recent experimental evidence has suggested that the development of hydration shells around metal oxides and chlorides can greatly increase the solubility of these metals, perhaps even to ore-forming concentrations (e.g., Archibald *et al.*, 2001, 2002). Support for the idea that aqueous vapour may play an important role in metal transport has also been provided by observations of high metal concentrations in vapour-rich fluid inclusions (Heinrich *et al.*, 1992, 1999), and the metal concentrations of fumarolic gases and sublimates (e.g., Symonds *et al.*, 1987, 1992; Wahrenberger *et al.*, 2002).

The underestimation of the importance of aqueous vapour in metal transport is also due to popular misconceptions regarding the nature of resurgent or second boiling during the exsolution of magmatic fluids. For example, it is commonly thought that second boiling produces a single phase (supercritical fluid) as opposed to coexisting aqueous liquid and vapour phases (Reynolds and Beane,

1985). However, as Sourirajan and Kennedy (1962) have shown, both the liquid and the vapour phases are stable at the salinity and pressure-temperature conditions of typical porphyry-epithermal ore-forming systems. It is also commonly assumed that if a vapour phase exsolves at all, it is a low density fluid, but at typical porphyry conditions (i.e., 600-700°C and 500-1000 bars), vapour has a relatively high density. An additional misconception is that the mass of the exsolving vapour is much smaller than that of the co-evolved liquid phase (Burnham, 1979), and is thus of little importance in metal transport, but a model proposed by Henley and McNabb (1978) demonstrated that the mass of an exsolving magmatic plume is vapour-dominated. Thus, several of the underlying assumptions for liquid-dominated metal transport are unfounded, and so the vapour phase should be more seriously considered as a transport agent in ore-forming processes.

1.2. Thermodynamic estimates of metal volatilities

As mentioned above, a number of studies have investigated the possibility that aqueous vapours might be capable of transporting metals in ore-forming concentrations. Several of these studies, however, have been based on thermodynamic calculations of metal volatility, i.e., the vapour pressure of the metallic species over the corresponding solid. For example, Krauskopf (1957, 1964) found that the volatility of $MoO_3(g)$, the *Mo* species thought to dominate magmatic vapours at 827°C, was about 30 ppm in water vapour, but decreased dramatically with temperature and oxygen fugacity. He therefore concluded that

orebody formation by deposition from an aqueous vapour was unlikely. Bernard *et al.* (1990) also investigated the solubility of *Mo* in an exsolved magmatic vapour, and produced similarly low results; for a sulphur-poor magmatic fluid at 680°C, the calculated *Mo* saturation concentration was 1 ppm, but this solubility decreased rapidly with temperature. Wood (1987) calculated the volatilities of the platinum group elements (PGE) in fluids at magmatic temperatures (527-1327°C), and concluded that, although the elements were soluble in vapour, the solubility was too low to explain the enrichment of PGE in mafic igneous deposits by vapour transport alone. The negligible metal solubilities predicted by these researchers may be attributed to the omission of hydrated species in the model parameters, as experimental studies have shown that the formation of such complexes greatly enhances solvation (e.g., Belton and Jordan, 1965; Archibald *et al.*, 2002).

1.3. Evidence of vapour transport from natural systems

Two lines of evidence for the vapour transport of metals are available in natural systems, namely the concentrations of metals in vapour-rich fluid inclusions from porphyry-epithermal ore deposits and the metal contents of fumarolic gases.

1.3.1. Fluid inclusion evidence

Fluid inclusion studies by Heinrich *et al.* (1992, 1999) and Ulrich *et al.* (1999, 2001) demonstrate that hydrothermal gases associated with the formation of porphyry copper-gold deposits contain more *Cu*, *Au* and *Mo* than the coexisting

brines. For example, *Cu* concentrations in vapour-rich fluid inclusions are on the order of about 3.3 and 1.2 weight percent (wt.%) at Grasberg (Indonesia) and Bajo de la Alumbrera (Argentina) deposits, respectively, whereas in the coexisting liquid-rich inclusions, the *Cu* concentrations are 0.76 and 0.30 wt.%. A similar level of *Cu* enrichment in the vapour was observed in fluid inclusions from the Mole Granite tin deposit, Australia. Gold was also preferentially concentrated in the Grasberg vapour (up to 10.17 ppm in the vapour-rich inclusions, but only up to 0.26 ppm in the coexisting liquids-rich inclusions), although this was not the case at Bajo de la Alumbrera, where vapour-rich inclusions only contained up to 0.53 ppm *Au* and the brine inclusions up to 0.79 ppm. The situation was reversed for molybdenum: vapour-rich inclusions at Bajo de la Alumbrera contain up to 300 ppm *Mo*, and the brine inclusions only about 70 ppm. At Grasberg, vapour-rich inclusions contain only 60 ppm *Mo*, whereas liquid-rich inclusions have *Mo* concentrations of about 600 ppm. These fluid inclusion data showed conclusively that copper was preferentially partitioned into the vapour phase, but suggest that gold and molybdenum were carried predominantly by either the liquid or the vapour, depending on the conditions.

1.3.2. *Fumarolic condensates and sublimates*

Analyses of fumarolic gas condensates indicate that aqueous vapour is capable of transporting appreciable amounts of molybdenum, and that *Mo* volatility is highly dependent on temperature. For example, condensates collected from 700°C fumarolic gases at the rhyolitic Satsuma Iwojima volcano (Japan) contain

between 0.4 and 0.9 ppm *Mo* (Hedenquist *et al.*, 1994). Similarly high concentrations have been reported for fumarolic condensates from the andesitic Merapi volcano (Indonesia) and the basaltic to andesitic Kudryavy volcano (Russia), i.e., 2.8 ppm for a 796°C fumarole and 0.27 ppm for a 920°C fumarole, respectively (Symonds *et al.*, 1987; Taran *et al.*, 1995; Wahrenberger *et al.*, 2002). For both volcanoes, the *Mo* content of the gases displayed an approximately linear increase with temperature. In comparison, fumarolic gases emitted from the basaltic Cerro Negro and Momotombo volcanoes (Nicaragua) contained 0.19-0.30 ppm and 0.07-0.50 ppm *Mo*, and were collected at 250-315°C and 470-860°C, respectively (Gemmell, 1987; Quisefit *et al.*, 1989). For these two volcanoes, there was no obvious correlation of *Mo* concentration with temperature, but this could reflect sampling and analytical errors that would have been enhanced by the very low metal concentrations of the gases. Condensates collected from low-temperature (495°C) fumaroles from the andesitic to dacitic White Island volcano (New Zealand) contained only about 3 ppb *Mo* (Tedesco and Toutain, 1991); the low *Mo* concentrations in these condensates may be attributed to the low temperature of the fumarolic gases.

This positive correlation of *Mo* solubility in the gas phase with temperature is expected, because the precipitation of *Mo* as molybdenite (MoS_2) or molybdenum oxides is sensitive to sharp decreases in temperature. This is supported by the distribution of fumarolic sublimates collected in silica tubes, in which *Mo*, largely deposited as molybdenite, precipitates exclusively at the high-

temperature (input) end of the tube. Molybdenite sublimates formed at temperatures between 550-650°C and 525-825°C have been collected from Kudryavy and Momotombo fumaroles, respectively; the relatively narrow temperature range indicates that *Mo* solubility in the fumarolic gases drops sharply as temperature is decreased (Wahrenberger *et al.*, 2002; Quisefit *et al.*, 1989). Similarly, maximum molybdenite deposition from Merapi fumaroles occurred over the temperature interval of 530-767°C (Symonds *et al.*, 1987). Sublimates collected from lower temperature gases did not contain molybdenite, indicating that the molybdenum load had been deposited as the gases cooled within the fumarolic vents. However, as the *Mo* is largely in the form of molybdenite, its solubility will also be dependent on the fugacity of H_2S (f_{H_2S} ; Bernard *et al.*, 1990). Molybdenite deposition temperatures from the gas phase have been shown to increase with increasing f_{H_2S} , which will limit the ability of S-rich fumarolic gases to carry *Mo*, especially in lower-temperature fumaroles. Generally, MoS_2 precipitates from fumarolic gases at low oxygen fugacities near those of the NNO or QFM reference buffers (Bernard *et al.*, 1990).

Molybdenite was the only *Mo*-bearing phase observed in the sublimates collected from fumaroles at Kudryavy, Momotombo, and Merapi volcanoes, but natural incrustations around the fumarolic vents contained other *Mo* minerals. At Kudryavy volcano, powellite ($CaMoO_4$) and ilsemannite ($MoO_3 \cdot nH_2O$) were deposited around fumarolic vents with gas temperatures of 650-750°C and 350-400°C, respectively (Wahrenberger *et al.*, 2002). Minor *Mo*-bearing minerals

precipitated around Kudryavy fumaroles consisted of tugarinovite (MoO_2) and molybdate (MoO_3), as reported by Bykova *et al.* (1995).

1.4. Experimental data in support of vapour transport of metals

Several recent experimental studies have measured the solubility of ore metals (Au , Ag , Cu , and Sn) in water vapour, and have investigated the corresponding metal speciation (Migdisov *et al.*, 1999; Archibald *et al.*, 2001, 2002; Migdisov and Williams-Jones, *submitted*). The experiments employed metal chlorides as starting materials, as the chloride complexes of the metals in question were thought to be the most soluble. These studies, conducted over a temperature range from 280 to 360°C and at pressures up to 144 bars, have shown that metal solubility increases with increasing f_{H_2O} , and that the metals, therefore, dissolve as hydrated gaseous complexes. The formation of these complexes augments metal solvation to such an extent that an appreciable amount of metal (up to 6.6 ppb Au , 101 ppb Ag , and 280 ppm Cu) can be transported in the vapour phase at physiochemical conditions encountered in nature. Similar experiments by Pokrovski *et al.* (2002) have shown that, at temperatures up to 500°C and pressures up to 600 bars, arsenious acid (H_3AsO_3) partitions preferentially into HCl and H_2S -bearing water vapour. The authors of this study attributed the high solubility of As to the formation of a gaseous arsenic hydroxide complex. The groundbreaking results of this research show conclusively that the vapour phase has an important role in ore-forming processes, and provide the impetus to extend this work to other metals and ligands. An obvious candidate for further

research is molybdenum, as reserves of this metal are largely found in porphyry deposits and associated hydrothermal systems, which are commonly vapour-dominated.

1.5. Molybdenum speciation in aqueous liquids

1.5.1. Pearson's HSAB principle

The behaviour of metals in aqueous liquids generally involves charged species, and can be predicted by Pearson's HSAB (Hard and Soft Acids and Bases) principle. Although charged species are not predicted to occur in gases, the behaviour of metals in aqueous liquids may serve as a guide to the interpretation of metal speciation in the gas phase. A general guideline for covalent and ionic bonding was established by Pearson (1963) based on the electrochemical and polarization characteristics of ions. Cations are considered to be Lewis acids, as they are acceptors of electrons, whereas electron-donating anions are considered to be Lewis bases. Lewis acids and bases are categorized as either hard or soft. Hard acids, which are small, highly charged metal ions, generally have a d^0 electron configuration and are, therefore, not easily deformed. Soft acids, on the other hand, are large metal ions with a low charge, and usually have a d^{10} electron configuration. Hard and soft bases are similarly defined.

Pearson's HSAB principle states that, in a competitive situation, hard acids prefer to complex with hard bases, and soft acids with soft bases (Pearson, 1963).

Thus, if a choice of ligands is available, metal ions will form complexes with ligands that bond in the same way. If no hard bases are available, however, a hard acid may be forced to bond with a borderline or soft base.

Under Pearson's classification, Mo^{6+} , Mo^{5+} , and Mo^{4+} are categorized as hard acids, but Mo^{6+} is harder than Mo^{5+} , and Mo^{5+} is harder than Mo^{4+} . Of the dominant ligands available in magmatic systems, OH , CO_3^{2-} , and F are considered to be hard bases, whereas Cl is borderline between hard and soft, and Br , CO , S^{2-} , H_2S , NH_3 , and SO_3^{2-} are soft bases. Among the hard ligands in magmatic systems, F is a minor constituent and is thus unlikely to be the dominant binder of Mo , but OH , CO_3^{2-} and Cl may be important.

1.5.2. Molybdenum speciation in hydrothermal liquids

Molybdenum speciation in supercritical hydrothermal fluids, especially at relatively low pressures, may imitate the behaviour of the metal in surficial or magmatic vapours. Glemser (1966) studied the reaction of MoO_3 with high-density water, and concluded that the metal was dissolved as oxyhydroxy complexes (e.g., $MoO_2(OH)_2$) at temperatures between 380-500°C and pressures from 65 to 3000 atm. Aqueous fluids at the low end of this pressure range may exhibit a vapour-like density, but those at 3000 atm have liquid-like characteristics. Similar aqueous Mo species were proposed in an experimental study by Smith *et al.* (1980), based on thermodynamic calculations of the Mo speciation in hydrothermal fluids at 250-350°C and 150 bars. These fluids were

slightly acidic and buffered by either magnetite-pyrite-pyrrhotite or nickel-nickel oxide-pyrite-pyrrhotite. The authors concluded that *Mo* is dissolved primarily as $HMoO_4^-(aq)$, with lesser amounts dissolved as $H_2MoO_4(aq)$, and could reach a maximum concentration of several thousand ppm. They also concluded that chlorine, fluorine, and sulphur *Mo* complexes are relatively unimportant in this system.

A comparable experiment was conducted by Cao (1989), in which the solubility of MoO_2 was measured in 0.0316 M to 5.7 M *NaCl* solutions at temperatures between 300 and 450°C and saturated water vapour pressure. As in the experiments of Smith *et al.* (1980), the solutions were slightly acidic, but were buffered by hematite-magnetite. Molybdenum solubility in this system was found to decrease with increasing f_{H_2S} , but to increase with increasing temperature, a_{NaCl} , and f_{O_2} , and reached 3000 ppm in sulphur-free solutions. The predicted *Mo* species included Mo^{5+} complexes such as $MoO(OH)Cl_2$ or $MoO(OH)_2Cl$, and Mo^{6+} species such as $HMoO_4^-$, $NaHMoO_4^0$, or $Na_2MoO_4^0$. However, as *NaCl* was used as the source of both Na^+ and Cl^- , it was difficult to distinguish the contributions of each ion to the *Mo* complex, and thus the proposed speciation is not well-supported (Wood and Samson, 1998).

As molybdenum is readily reduced in hydrothermal solutions (Wood and Samson, 1998), the aqueous species comprising *Mo(VI)*, *Mo(V)*, and *Mo(IV)* are, in principle, all plausible. According to the HSAB principle, *Mo* in all of these

oxidation states should behave as a hard acid, thus oxide, oxyacid or oxyhydroxy complexes are expected. The chloride ligand, being borderline between hard and soft bases, may be expected to complex with *Mo* only under unusual conditions e.g., in highly acidic, high-salinity, reducing fluids (Wood and Samson, 1998).

1.5.3. Molybdenum hydrate stability in aqueous and acidic liquids

As previous studies have found that the development of hydration shells can substantially increase metal solvation, the behaviour of hydrated *Mo* species in low-density liquids is also of interest. Huttig and Kurre (1923) determined that the stability of *Mo* hydrates in aqueous solutions is sensitive to temperature, which indicates that gaseous *Mo* hydrates may also have a limited range of stability. These authors found that the *Mo* dihydrate, $MoO_3 \cdot 2H_2O(aq)$, is stable only below 40°C, and will convert to the monohydrate upon heating. Ferris (1961), however, determined that a reversion of mono- to dihydrate does not occur upon the cooling of an aqueous solution from 55 to 26°C. Although these authors use a different nomenclature for the aqueous *Mo* complexes, the species discussed are the same as the molybdic acids predicted to form in hydrothermal supercritical fluids; Freedman (1963) and Tytko *et al.* (1987) proposed that when dissolved in aqueous liquid, *Mo* hydrates are more appropriately referred to as the corresponding molybdic acids.

Change in pH is also instrumental in destabilizing dissolved *Mo* hydrates. As surficial and magmatic vapours are generally highly acidic, the stability of *Mo*

hydrates at low pH is also of some importance in gas-phase speciation predictions. Ferris (1961) determined that in acidic solutions between 26 and 55°C, the solubility of both *Mo* trioxide and the dihydrate increase with decreasing pH. At nitric acid concentrations higher than 3M, however, the solubility of $MoO_3 \cdot 2H_2O$ decreases with increasing acidity. Likewise, in solutions of $MoO_3 \cdot H_2O$ with a nitric acid concentration greater than 2-3M, the solubility of the monohydrate decreases and precipitates as the yellow dihydrate (Cannon, 1959; Ferris 1961). Depending on the type of acid, a decrease in solubility with increasing acidity may not occur. Cannon (1959) investigated the effects of *HCl*, *HNO₃*, and *H₃PO₄* on the solubility of $MoO_3 \cdot H_2O(aq)$ at 20°C, and determined that its solubility reaches a maximum at 3.81M *HNO₃* or 3.90M *H₃PO₄*, but no such peak was observed when the compound was dissolved in *HCl*. This author suggested that the hydrate forms an oxychloride, $MoO(OH)Cl_2(aq)$, when combined with hydrochloric acid, indicating that *Mo* hydrate solubility is a function of aqueous speciation as well as pH. As *HCl* is the predominant strong acid in magmatic systems, both the oxychloride and the hydrate may be important *Mo* species.

1.6. Gaseous molybdenum speciation

1.6.1. Molybdenum volatility in dry systems

The volatility of *Mo* in dry systems may be considered to represent the minimum solubility of *Mo* species in the vapour phase, and may assist with interpretation of

Mo speciation in aqueous vapour. Berkowitz *et al.* (1957) measured partial pressures of $(\text{MoO}_3)_3(g)$ over $\text{MoO}_3(s)$ for three species: $(\text{MoO}_3)_3$, $(\text{MoO}_3)_4$, and $(\text{MoO}_3)_5$. Of the three, the trimer, $(\text{MoO}_3)_3(g)$, was found to be the dominant *Mo* species, and had partial pressures ranging from 1.66×10^{-6} to 1.27×10^{-4} bars as temperature increased from 588 to 700°C. Ikeda *et al.* (1983) found that the partial pressure of $\text{MoO}_3(g)$ over solid *Mo-MoO*₂ increased from 10^{-7} to 10^{-5} bar with a temperature increase from 1280 to 1480°C. The dioxide, MoO_2 , and the polymeric species $(\text{MoO}_3)_2$ and $(\text{MoO}_3)_3$, had lower partial pressures than MoO_3 . When measured over solid MoO_3 , however, $(\text{MoO}_3)_3(g)$ had a partial pressure of roughly 10^{-6} bar at 540°C, and of 4×10^{-5} bar at 680°C. Ikeda *et al.* (1983) also demonstrated that the partial pressures of various *Mo* oxides increased with f_{O_2} . With increasing oxygen pressure from 10^{-30} to 10^{-10} bar and P_{MoO_x} from 10^{-25} to 10^{-5} bar, the dominant gaseous *Mo* species at 727°C changed in succession from MoO_2 to MoO_3 , $(\text{MoO}_3)_2$, $(\text{MoO}_3)_3$, the intermediate phase $\text{MoO}_4\text{O}_{11}$, and then to $(\text{MoO}_3)_4$, so it is possible that polymeric *Mo* hydrates may exist at high f_{O_2} in water vapour. Blackburn *et al.* (1958) found that upon vapourization at 727-1027°C, much of MoO_2 disproportionates to $\text{MoO}_3(g)$ and $\text{Mo}(s)$ instead of forming $\text{MoO}_2(g)$, suggesting that MoO_3 is more volatile than MoO_2 at these conditions. Thus, over a broad range of temperatures, the *Mo(VI)* trioxides appear to be more volatile than *Mo(IV)* dioxide.

1.6.2. Thermodynamic modeling

Mathematic models of multi-component systems have been employed to determine the metal speciation of molybdenum-bearing fumarolic gases. Closed-system cooling calculations based on the fumarolic gases of Kudryavy volcano were used by Wahrenberger *et al.* (2002) to predict the major volatile trace element species in a vapour containing the elements C, O, H, S, Cl, Br, F, and I, in equilibrium with a condensed phase. These calculations were done using a simple volatility model (GASTHERM; Symonds and Reed, 1993), and thus did not take into account the possible formation of hydration shells around the metallic species. The model predicted that $MoCl_2O_2(g)$ is the dominant Mo complex at temperatures between 300-375°C, and that $H_2MoO_4(g)$ predominates at temperatures between 375-1000°C. The latter species may be better described as $MoO_3 \bullet H_2O$, as Freedman (1963) and Tytko *et al.* (1987) opined that the monomeric molybdic acid, H_2MoO_4 , exists only in aqueous solutions. Wahrenberger *et al.* (2002) reported the mole fractions of gaseous $MoCl_2O_2$ and H_2MoO_4 in their simulated system as 10^{-14} to 10^{-17} (5.3×10^{-5} - 5.3×10^{-8} ppb) and 10^{-7} to 10^{-14} (530 - 5.3×10^{-5} ppb), respectively. The predicted metal concentrations at the low end of the temperature range, however, were considerably lower than those measured in the corresponding fumaroles.

SOLVGAS and GASWORKS models (Symonds *et al.*, 1987) of the more chlorine-rich gases of the andesitic to dacitic Augustine volcano (Alaska), have suggested that MoO_2Cl_2 is the most stable Mo species, except at very high

temperatures, i.e. above 940°C, where $H_2MoO_4(g)$ predominates (Symonds *et al.*, 1992). The mole fraction of MoO_2Cl_2 was calculated as 1.1×10^{-7} (590 ppb), and that of H_2MoO_4 as 6.5×10^{-8} (350 ppb), for a temperature of 870°C.

Thermodynamic modeling of Mt. St. Helens and Kilauea gases, also using SOLVGAS, produced similar results (Bernard *et al.*, 1990). These calculations suggested that H_2MoO_4 is the dominant gaseous species at temperatures above 320° and 400°C for Mt. St. Helens and Kilauea gases, respectively. $MoO_2Cl_2(g)$ was predicted to be the dominant species at lower temperatures and for very high HCl fugacities (10 mole %, which is very rare in geologic systems). Mount St. Helens and Kilauea gases typically contain 95 and 85 ppb Mo , respectively, and the concentrations predicted by the SOLVGAS model were roughly 50 ppb (i.e., above the MoO_2Cl_2 -dominated temperature range, $f_{H_2MoO_4} = 10^{-8}$, and independent of temperature). These authors also predicted that a sulphur-poor, gas-like supercritical fluid at about 680°C has a Mo saturation level of about 1 ppm, which is comparable to the Mo concentrations measured in fumarolic condensates. Increased oxygen fugacities caused no change in the dominant Mo complexes, but did cause the predicted fugacities of molybdenum(IV) and molybdenum(II) oxides to decrease. Similarly, at high HF and HBr fugacities, $H_2MoO_4(g)$ and $MoO_2Cl_2(g)$ were still predominant. Increased H_2S fugacity did not affect the dominant gaseous species, but did promote deposition of MoS_2 . Comparison of these results with those of Wahrenberger *et al.* (2002) and Symonds *et al.* (1987, 1992) suggests that gaseous Mo speciation varies with

gas composition and temperature, but that the hydrated molybdenum trioxide or molybdic acid is an important complex even in gases with relatively high chlorine concentrations.

1.6.3. Partitioning of Mo between magmas and aqueous fluid

Thermodynamic predictions of molybdenum speciation concur with investigations of the partitioning of molybdenum between silicate magmas and the exsolving magmatic vapour. Candela and Holland (1981, 1984) have shown that at 750°C and 1.4 kbar, $D_{Mo}^{f/m}$ (f = supercritical fluid, m = melt) is independent of fluorine concentration up to at least 1.7 wt.%, and of chlorine up to about 0.16 wt.%. These authors therefore concluded that Mo oxyhydroxides such as $MoO_2(OH)_2(g)$ are the dominant species up to these conditions. Tingle and Fenn (1984) observed that $D_{Mo}^{f/m}$ was independent of fluorine concentration at 1000°C and 1 kbar. However, at higher fluorine concentrations, and temperature and pressure conditions of 750°-800°C and 1-4 kbar, Bai and Koster van Groos (1999) observed a decrease in $D_{Mo}^{f/m}$. They therefore suggested that the presence of fluorine may decrease $D_{Mo}^{f/m}$ by depolymerizing the melt and increasing the number of sites available for Mo within the melt framework. They also reported an increase in $D_{Mo}^{f/m}$ at high concentrations of HCl, which was probably due to the formation of gaseous Mo-chloride complexes.

Thus, molybdenum speciation predictions from thermodynamic and experimental considerations concur well with the HSAB principle. The hydroxide ion is the

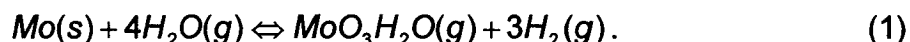
most likely to form complexes with *Mo* over a broad range of temperatures but only under alkaline conditions, whereas the borderline ligand, *Cl*, may form *Mo* complexes only at low temperatures and/or high *HCl* fugacities. Of the other hard ligands, *F* is a minor component in magmatic systems, and was shown by thermodynamic calculations and partitioning experiments to be an unimportant ligand for *Mo*. Significantly, both gaseous species proposed to be predominant in magmatic systems (H_2MoO_4 and MoO_2Cl_2) are *Mo(VI)* complexes, suggesting that *Mo(VI)* species are more soluble than those of *Mo* in other oxidation states. Also, as the high temperatures and pressures of the partitioning experiments likely gave rise to a supercritical fluid with liquid- rather than vapour-like characteristics, molybdenum speciation in the liquid phase may be comparable to that in the vapour phase. It thus appears as though the speciation of *Mo* remains broadly similar in fluids over a wide range of temperature, pressure, and composition, and that the favoured species under most of these conditions is either the molybdic acid or hydrate. This preferred speciation across multiple systems is strong grounds for the suggestion that *Mo* hydrate may be the gas-phase complex in ore-forming environments.

1.6.4. Experimental data in support of the vapour transport of Mo

Early experimental studies suggested that *Mo* forms hydrated complexes in aqueous vapour, and that the formation of these complexes causes an appreciable increase in *Mo* solubility. From measurements of the mass of *Mo* trioxide precipitated from a stream of 600-700°C water vapour, Millner and

Neugebauer (1949) observed that the volatility of MoO_3 increased with P_{H_2O} and temperature, and suggested that Mo dissolves as $MoO_3 \cdot H_2O(g)$. Elliot (1952) and Sardi (1963) observed a similar dependence between 550-560°C and 580-730°C, respectively, and came to the same conclusion regarding speciation. However, as Millner and Neugebauer (1949) and Elliot (1952) reported only four and three data points, respectively, and as the experiments of Sardi (1963) did not attain equilibrium, the stoichiometry of the dissolved complex was not confirmed.

Belton and Jordan (1965), using a weight-loss method, later determined the stoichiometry of the Mo monohydrate at temperatures from 1200-1500°C and water vapour pressures from 0.04-0.5 bars. These researchers observed an increase in the apparent vapour pressure of Mo with P_{H_2O} , and used a ratio of water vapour to pure hydrogen gas to calculate the number of oxygen atoms in the Mo species, based on the reaction:



They determined that possible gaseous species include $MoO_2 \cdot H_2O$, $MoO_4 \cdot H_2O$ and $MoO_3 \cdot H_2O$, but that the vapour pressures of the two former species were lower than the latter. The hydrated trioxide was thus considered to be the most important Mo complex in aqueous vapour. The apparent vapour pressures of this complex at the conditions of the experiment were between 1.67×10^{-5} and 1.338×10^{-3} bars (1.0-12.8 g/L), increasing with temperature.

Several researchers have, therefore, concluded that *Mo* forms a monohydrate trioxide in aqueous vapour. However, the experiments by Millner and Neugebauer (1949), Elliot (1952), and Sardi (1963) did not identify the stoichiometry of the hydrated complex, and thus the hydration number is unknown at temperatures below those employed by Belton and Jordan (1965). As the behaviour of molybdenum at the temperature and pressure conditions of porphyry-hydrothermal systems is of interest, further investigation of the solubility of *Mo* in water vapour is required.

1.7. Objectives of the study

The overall objectives of this study were:

- (1) To measure the solubility of molybdenum in water vapour as a function of temperature and f_{H_2O} ;
- (2) To determine the nature of the resulting *Mo* species, and;
- (3) To establish whether magmatic vapours could play a significant role as an agent of metal transport during the formation of porphyry *Mo* deposits.

As previous studies indicate that *Mo(VI)* is more volatile than molybdenum in other oxidation states, the experiments were conducted with MoO_3 . Moreover, as *Mo* is most soluble in aqueous liquids as a hydrate or oxyacid, H_2O served as both solvent and ligand. The potential of water vapour to be an ore fluid for porphyry *Mo* deposits was evaluated by extrapolating the experimentally-

determined *Mo* solubilities to typical porphyry conditions (i.e., 600°C, 500 bars, and f_{O_2} and f_{S_2} consistent with the hematite-magnetite-pyrite buffer) and calculating the time required to form a high-grade molybdenum orebody, assuming H_2O fluxes estimated for fumaroles at an actively degassing volcano (i.e., Satsuma-Iwojima volcano, Japan, with an average H_2O flux of 5 million tonnes per year).

1.8. Thesis organization

This thesis is divided into three chapters: a general introduction, followed by a stand-alone manuscript, and a general conclusion. In the second chapter, I report the results of an experimental investigation of the solubility and speciation of molybdenum in water vapour at temperatures from 300 to 360°C and pressures from 48 to 163 bars.

The experiments were based on the methodology of Migdisov *et al.* (1999) for the *AgCl-HCl-H₂O* system, and involved the following steps: Titanium autoclaves were charged with powdered *MoO₃* packed into quartz glass ampoules and suspended within quartz glass holders. Pre-determined volumes of liquid water in the autoclaves controlled the water vapour pressure of the system. Once charged, the autoclaves were heated in an oven at temperatures from 300° to 360°C until equilibrium was reached (6 days at 320°C). The system was then

quenched, and the resulting condensate was analyzed for *Mo* concentration by ICP-MS.

Molybdenum concentrations were used to predict gaseous speciation and to derive equilibrium constants for the hydrated MoO_3 species. The equilibrium constants were then used to evaluate the importance of the vapour in transporting *Mo* during the formation of *Mo* porphyry deposits. In order to estimate the time required for a *Mo* porphyry deposit to form via vapour transport, the equilibrium constant for the formation of the hydrated *Mo* species was extrapolated to a temperature of 600°C and a pressure of 500 bars, and the solubility of MoO_3 in equilibrium with MoS_2 was calculated. The oxygen and sulphur fugacities were those in equilibrium with the assemblage hematite-magnetite-pyrite. The calculations indicate that the amount of molybdenum transported in the vapour is sufficient to produce a *Mo* deposit comparable in size to the Endako *Mo* deposit, B.C. (336 Mt with an average grade of 0.087% *Mo*) in about 900,000 years, which is within the lifetime of some geothermal systems (Christiansen, 1984).

1.9. References

- Archibald, S.M., Migdisov, A.A. and Williams-Jones, A.E. (2001) The stability of Au-chloride complexes in water vapor at elevated temperatures and pressures. *Geochim. Cosmochim. Acta* 65: 4413-4423.
- Archibald, S.M., Migdisov, A.A. and Williams-Jones, A.E. (2002) An experimental study of the stability of copper chloride complexes in water vapor at elevated temperatures and pressures. *Geochim. Cosmochim. Acta* 66: 1611-1619.
- Bai, T.B. and Koster van Groos, A.F. (1999) The distribution of Na, K, Rb, Sr, Al, Ge, Cu, W, Mo, La, and Ce between granitic melts and coexisting aqueous fluids. *Geochim. Cosmochim. Acta* 63: 1117-1131.
- Belton, G.R. and Jordan, A.S. (1965) The volatilization of molybdenum in the presence of water vapor. *J. Phys. Chem.* 69: 2065-2071.
- Berkowitz, J., Inghram, M.G. and Chupka, W.A. (1957) Polymeric gaseous species in the sublimation of molybdenum trioxide. *J. Chem. Phys.* 26: 842-846.
- Bernard, A., Symonds, R.B. and Rose, W.I., Jr. (1990) Volatile transport and deposition of molybdenum, tungsten, and rhenium in high-temperature magmatic fluids. *Applied Geochem.* 5: 317-326.
- Blackburn, P.E., Hoch, M. and Johnston, H.L. (1958) The vaporization of molybdenum and tungsten oxides. *J. Phys. Chem.* 62: 769-773.

- Burnham, C.W. (1979) Magmas and hydrothermal fluids. In: *Geochemistry of Hydrothermal Ore Deposits*, 2nd Edition. Ed: H.L. Barnes. John Wiley & Sons, Toronto, 798 pp.
- Bykova, E.Y., Znamenskii, V.S., Kovalenker, V.A., Marsii, I.M. and Baturin, S.V. (1995) Associations and conditions for molybdenum mineral deposition in exhalation products of the Kudryavyi volcano, Iterup, the Kuril Islands. *Geologiya Rudnykh Mestorozhdenii* 37: 265-273.
- Candela, P.A. and Holland, H.D. (1981) The effect of fluorine on the partitioning of molybdenum between a magma and a hydrothermal fluid. *Geol. Soc. Amer. Abstr. Prog.* 13: 422.
- Candela, P.A. and Holland, H.D. (1984) The partitioning of copper and molybdenum between silicate melts and aqueous fluids. *Geochim. Cosmochim. Acta* 48: 373-380.
- Cannon, P. (1959) Solubility of molybdenum trioxide in various mineral acids. *J. Inorg. Nucl. Chem.* 11: 124-127.
- Cao, X., Richardson, S.M. and Richardson, C.K. (1989) Experimental studies of the hydrothermal transport and deposition of molybdenum. *Abstr. Prog. Geol. Soc. Am.* 21: 150.
- Christiansen, R.L. (1984) Yellowstone magmatic evolution: its bearing on understanding large-volume explosive volcanism. In: *Studies in Geophysics: Explosive Volcanism: Inception, Evolution, and Hazards*. National Academic Press, Washington, D.C., pp. 84-95.

- Elliot, R.B. (1952) Gaseous hydrated oxides, hydroxides, and other hydrated molecules. *University of California, Radiation Laboratory Report* 1831, 52 pp.
- Ferris, L.M. (1961) Solubility of molybdic oxide and its hydrates in nitric acid, nitric acid-ferric nitrate, and nitric acid-uranyl nitrate solutions. *J. Chem. Eng. Data* 6: 600-603.
- Freedman, M.L. (1963) The state of molybdenum(VI) in perchloric acid solutions. *J. Inorg. Nucl. Chem.* 25: 575-580.
- Gemmell, J.B. (1987) Geochemistry of metallic trace elements in fumarolic condensates from Nicaraguan and Costa Rican volcanoes. *J. Volcanol. Geotherm. Res.* 33: 161-181.
- Glemser, O., Stoecker, U. and Wendlandt H.G. (1966) Reaction of solid oxides with high density water at high temperatures. *Berichte der Bunsen-Gesellschaft* 70: 1129-1134.
- Hedenquist, J.W., Aoki, M. and Shinohara, H. (1994) Flux of volatiles and ore-forming metals from the magmatic-hydrothermal system of Satsuma Iwojima volcano. *Geology* 22: 585-588.
- Heinrich, C.A., Ryan, C.G., Mernagh, T.P. and Eadington, P.J. (1992) Segregation of ore metals between magmatic brine and vapor: a fluid inclusion study using PIXE Microanalysis. *Econ. Geol.* 87: 1566-1583.
- Heinrich, C.A., Günther, D., Audétat, A., Ulrich, T. and Frischknecht, R. (1999) Metal fractionation between magmatic brine and vapor, determined by microanalysis of fluid inclusions. *Geology* 27: 755-758.

- Henley, R.W. and McNabb, A. (1978) Magmatic vapor plumes and ground-water interaction in porphyry copper emplacement. *Econ. Geol.* 73: 1-19.
- Huttig, G.V. and Kurre, B. (1923) The hydrates of molybdenum trioxide. *Z. Anorg. Allgem. Chem.* 126: 167-175.
- Ikeda, Y., Ito, H., Mizuno, T., Amioka, K. and Matsumoto, G. (1983) Sublimation behavior of molybdenum oxide. *High Temp. Sci.* 16: 1-22.
- Krauskopf, K.B. (1957) The heavy metal content of magmatic vapor at 600°C. *Econ. Geol.* 52: 786-807.
- Krauskopf, K.B. (1964) The possible role of volatile metal compounds in ore genesis. *Econ. Geol.* 59: 22-45.
- Migdisov, A.A., Williams-Jones, A.E. and Suleimenov, O.M. (1999) Solubility of chlorargyrite (AgCl) in water vapor at elevated temperatures and pressures. *Geochim. Cosmochim. Acta* 63: 3817-3827.
- Migdisov, A.A. and Williams-Jones, A.E. An experimental study of cassiterite solubility in HCl-bearing water vapor. (*submitted*)
- Millner, T. and Neugenbauer, J. (1949) Volatility of the oxides of tungsten and molybdenum in the presence of water vapour. *Nature* 163: 601-602.
- Pearson, R.G. (1963) Hard and soft acids and bases. *Physical and Inorganic Chemistry* 85: 3533-3539.
- Pokrovski, G.S., Zakirov, I.V., Roux, J., Testemale, D., Hazemann, J.-L., Bychkov, A.Y. and Golikova, G.V. (2002) Experimental study of arsenic speciation in vapour phase to 500°C: Implications for As transport and

- fractionation in low-density crustal fluids and volcanic gases. *Geochim. Cosmochim. Acta* 66: 3453-3480.
- Quisefit, J.P., Toutain, J.P., Bergametti, G., Javoy, M., Cheynet, B. and Person, A. (1989) Evolution versus cooling of gaseous volcanic emissions from Momotombe Volcano, Nicaragua: thermochemical model and observations. *Geochim. Cosmochim. Acta* 53: 2591-2608.
- Reynolds, T.J. and Beane, R.E. (1985) Evolution of hydrothermal fluid characteristics at the Santa Rita, New Mexico porphyry deposit. *Econ. Geol.* 80: 1328-1347.
- Sardi, A. (1963) Reduction of Mo trioxide II. Appearance of oxides phases between Mo trioxide and Mo dioxide during reduction of Mo trioxide by a flowing gas mixture containing H and water. *Acta Chim. Acad. Sci. Hung.* 39: 145-160.
- Smith, R.W., Norman, D.I. and Popp, C.J. (1980) Calculated solubility of molybdenite in hydrothermal solutions. *Abstr. Prog. Geol. Soc. Am.* 12: 525.
- Sourirajan, S. and Kennedy, G.C. (1962) The system H₂O-NaCl at elevated temperatures and pressures. *Am. J. Sci.* 260: 115-141.
- Symonds, R.B., Rose, W.I., Reed, M.H., Lichte, F.E. and Finnegan, D.L. (1987) Volatilization, transport, and sublimation of metallic and non-metallic elements in high temperature gases at Merapi Volcano, Indonesia. *Geochim. Cosmochim. Acta* 51: 2083-2101.

- Symonds, R.B., Reed, M.H. and Rose, W.I. (1992) Origin, speciation, and fluxes of trace-element gases at Augustine volcano, Alaska: insights into magma degassing and fumarolic processes. *Geochim. Cosmochim. Acta* 56: 633-657.
- Symonds, R.B. and Reed, M.H. (1993) Calculation of multicomponent chemical equilibria in gas-solid-liquid systems – Calculation methods, thermochemical data, and applications to studies of high-temperature volcanic gases with examples from Mount St-Helens. *Am. J. Sci.* 293: 758-864.
- Taran, Y.T., Hedenquist, J.W., Korzhinsky, M.A., Tkachenko, S.I. and Shmulovich, K.I. (1995) Geochemistry of magmatic gases from Kudryavy volcano, Iturup, Kuril Islands. *Geochim. Cosmochim. Acta* 59:1749-1761.
- Tedesco, D. and Toutain, J.P. (1991) Chemistry and emission rate of volatiles from White Island volcano (New Zealand). *Geophys. Res. Lett.* 18: 113-116.
- Tingle, T.N. and Fenn, P.M. (1984) Transport and concentration of molybdenum in granite molybdenum systems: effects of fluorine and sulfur. *Geology* 12: 156-158.
- Tytko, K.H., Baethe, G. and Mehmke, K. (1987) What is “molybdic acid” or “polymolybdic acid”? *Z. Anorg. Allgem. Chem.* 555: 98-108.
- Ulrich, T., Gunther, D. and Heinrich, C.A. (1999) Gold concentrations of magmatic brines and the metal budget of porphyry copper deposits. *Nature* 399: 676-679.

- Ulrich, T., Gunther, D. and Heinrich, C.A. (2001) Evolution of a porphyry Cu-Au deposit, based on LA-ICP-MS analysis of fluid inclusions: Bajo de la Alumbrera, Argentina. *Econ. Geol.* 96: 1743-1762.
- Wahrenberger, C., Seward, T.M. and Dietrich, V. (2002) Volatile trace-element transport in high-temperature gases from Kudryavy volcano (Iturup, Kurile Islands, Russia). In: *Water-Rock Interactions, Ore Deposits, and Environmental Geochemistry: A Tribute to David A. Crerar*. Eds. Roland Hellmann and Scott A. Wood. The Geochemical Society, Special Publication No. 7, pp. 307-327.
- White, W.H., Bookstrom, A.A., Kamilli, R.J., Ganster, M.W., Smith, R.P, Ranta, D.E. and Steininger, R.C. (1981) Character and origin of Climax-type molybdenum deposits. *Econ. Geol.* 75th Anniversary Volume: 270-316.
- Wood, S.A. (1987) Thermodynamic calculations of the volatility of the platinum group elements (PGE): the PGE contents of fluids at magmatic temperatures. *Geochim. Cosmochim. Acta* 51: 3041-3050.
- Wood, S.A. and Samson, I.M. (1998) Solubility of ore minerals and complexation of ore metals in hydrothermal solutions. In: *Techniques in Hydrothermal Ore Deposit Geology*. Eds. Jeremy P. Richards and Peter B. Larson. *Reviews in Economic Geology* v. 10, pp. 33-80.

Introduction to Chapter 2

In the preceding chapter, a review of data pertaining to the behaviour of molybdenum in aqueous liquids and gases was presented, and served to support the idea that the vapour phase may play an important role in the transport of *Mo*.

In Chapter 2, experimental data from an investigation of the solubility of *Mo* in water vapour is reported, and a speciation scheme for gaseous *Mo* complexes is proposed. The data are then used to develop a model for the formation of *Mo* porphyry deposits.

CHAPTER 2

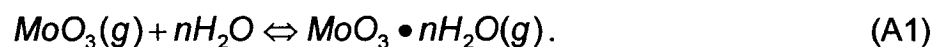
THE SOLUBILITY AND SPECIATION OF MOLYBDENUM IN WATER VAPOUR AT ELEVATED TEMPERATURES AND PRESSURES: IMPLICATIONS FOR ORE GENESIS

K.U. Rempel¹, A.A. Migdisov¹, and A.E. Williams-Jones¹

¹*McGill University, 3450 University St., Montreal, Quebec H3A 2A7*

2.1. Abstract

The solubility of molybdenum trioxide in liquid-undersaturated water vapour has been investigated experimentally at 300, 320, and 360°C and 48 to 163 bars. Results of these experiments show that the solubility of MoO_3 in the vapour phase is between 1 and 23 ppm, which is 19-20 orders of magnitude higher than that in a water-free system. Molybdenum solubilities increase linearly with f_{H_2O} , indicating that the metal forms a gaseous hydrated complex of the type $MoO_3 \cdot nH_2O$ by the reaction:



The hydration number, n , is interpreted to have a value of 2.6 at 300°C, 2.5 at 320°C, and 3.0 at 360°C. Values of $\log K$ for this reaction are 16.9 at 300°C, 16.5 at 320°C, and 12.5 at 360°C.

Calculations based on the extrapolated solubility of MoO_3 in equilibrium with molybdenite at 600°C and 500 bars, using average H_2O and total S fluxes of actively degassing volcanoes, with f_{O_2} and f_{S_2} controlled by the assemblage hematite-magnetite-pyrite, indicate that the vapour phase can transport sufficient Mo in about 900,000 years (within the life of some geothermal systems) to form a deposit of 336 Mt, with an average grade of 0.087% Mo (e.g., the Endako Mo -porphyry deposit, Canada).

2.2. Introduction

Although conventional models for the formation of porphyry *Cu-Mo* deposits assume that metals are transported by an aqueous liquid (e.g., Burnham, 1979; Reynolds and Beane, 1985), a small number of researchers have proposed that the vapour phase may also play an important role in metal transport, as vapour commonly dominates the hydrothermal system in porphyry settings (e.g., Henley and McNabb, 1978; Eastoe, 1982). This latter idea has recently gained credibility as a result of studies reporting elevated concentrations of metals in vapour-rich fluid inclusions (Heinrich *et al.*, 1992, 1999; Ulrich *et al.*, 1999). For example, Ulrich *et al.* (1999) have shown that at the Bajo de la Alumbrera *Cu-Mo-Au* porphyry deposit, Argentina, *Cu* and *Mo* concentrations in vapour-rich inclusions reach 1.2 wt.% and 300 ppm, respectively, whereas their concentrations in the coexisting brine are 0.30 wt.% and 70 ppm, respectively. Significantly, metal-bearing condensates and sublimates collected from fumarolic gases are also commonly reported to contain high concentrations of metals, e.g., up to 2.8 ppm *Mo* in 800°C fumaroles at Merapi volcano, Indonesia (Symonds *et al.*, 1987). Further support for the idea that the vapour phase can act as an agent of metal transport in hydrothermal systems is provided by experimental studies which have shown that, at temperatures from 280 to 360°C and pressures up to 144 bars, metals such as *Cu* and *Au* can dissolve in *H₂O-HCl* vapours in concentrations similar to those required for ore-forming fluids (Archibald *et al.*, 2001, 2002; Williams-Jones *et al.*, 2002). The solubilities of these metals

increase exponentially with water fugacity, which led these researchers to conclude that the metals were forming gaseous hydrated complexes.

In this paper, we report the results of experiments designed to measure the solubility of molybdenum oxide in water vapour as a function of temperature and f_{H_2O} . We then go on to use these data to determine the speciation of *Mo* in water vapour and employ extrapolated formation constants for these species to estimate of the time required to form a *Mo* porphyry deposit under physicochemical conditions typical of porphyry *Mo* systems.

2.3. Experimental method

The experimental method employed in this study is based on that of Migdisov *et al.* (1999) for the *AgCl-HCl-H₂O* system. Experiments were performed in autoclaves constructed of titanium alloy (Grade 2 ASTM B348), the inner surfaces of which were preconditioned with nitric acid to produce a protective layer of *TiO₂*. Before loading, autoclave volumes were measured by filling with 25°C nanopure[®] water from a beaker and weighing the beaker before and after filling. These measured volumes were then used to calculate the water vapour pressure of the system. As the vapour pressure of *MoO₃* is negligible compared to that of *H₂O*, the total pressure of the system was assumed to be equal to that of water vapour.

Autoclaves were loaded with powdered molybdenum(VI) oxide (Alfa Aesar, 99.9995% purity) which was placed in open quartz glass ampoules, packed with porous quartz glass wool at either end. Runs buffered for f_{O_2} employed an additional ampoule of powdered MoO_2 (Alfa Aesar, 99% purity). The ampoules were supported inside the autoclaves by quartz glass holders, which served to suspend the powdered molybdenum oxide above the solvent at the start of the experiment. The latter consisted of between 2.0 and 10.0 mL of nanopure[®] water, which was pipetted into the bottom of the autoclave, and represented amounts calculated to produce dry vapour at the conditions of the experiment. The experimental apparatus is shown schematically in figure 1.

For experiments conducted at 300° and 320°C, autoclaves were heated in a Fisher Isotemp[®] forced-draft oven (model 838F). A Barnstead Thermolyne muffle furnace (model 30400) was used for experiments at 360°C. In order to reduce thermal gradients, autoclaves were placed inside aluminum boxes with wall thicknesses of 1.5 cm and 0.5 cm for the low temperature and high temperature experiments, respectively. At the completion of each experiment, the autoclaves were quenched in a cold water bath until room temperature was attained. After quenching, the autoclaves were opened, the quartz glass holders and ampoules were removed and 1 mL of hydrochloric acid (Optima[®] grade, Fisher Scientific) was added to dissolve any precipitate on the autoclave walls. The walls were then washed 50-60 times with 1 mL aliquots of the resulting solution to ensure that any Mo on the sides of the autoclave was collected. The condensate was

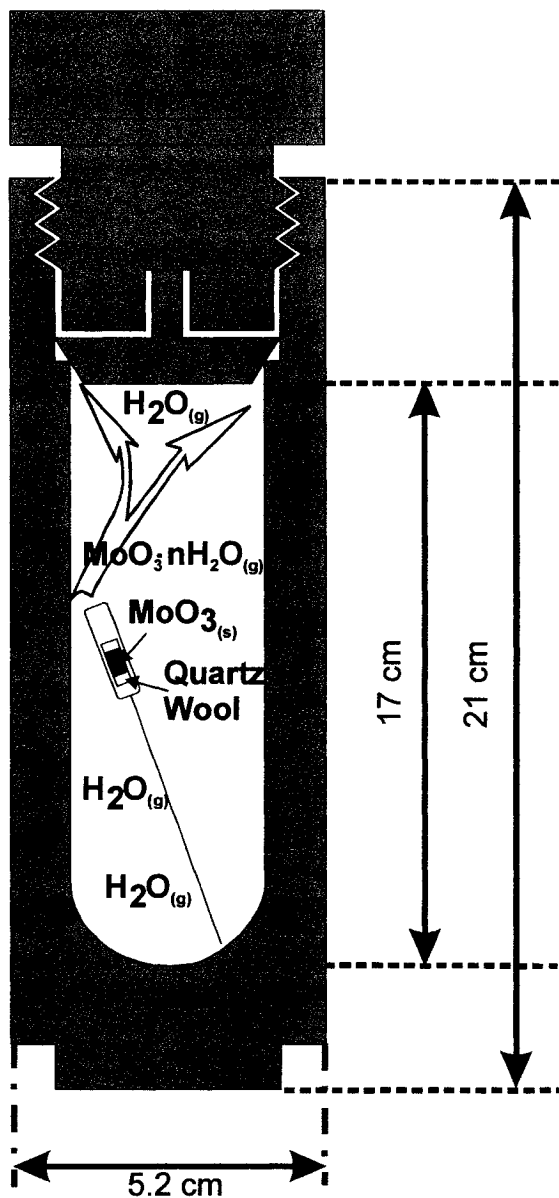


Figure 1: Schematic diagram of the titanium autoclaves employed in the experiments. The autoclaves are constructed of Grade II ASTM B348 titanium alloy, and the interiors are preconditioned with nitric acid to provide a protective coating of TiO_2 .

then pipetted into a clean plastic test tube, sealed, and weighed. Molybdenum concentrations in the condensates were analyzed by ICP-MS; the detection limit was 0.1 ppb.

There are two potentially important sources of error in these experiments. The first is irreversible deposition of *Mo* on the cold parts of the autoclaves (the walls) due to temperature gradients in the ovens, and would be evident as anomalously high *Mo* concentrations in the run condensates. The second source of error results from the partitioning of *Mo* from the vapour phase into the liquid during heating or quenching of the autoclaves, and would produce exceptionally high *Mo* concentrations in the condensates (as *Mo* is much more soluble in the liquid than in the vapour). Transport of *Mo* onto the autoclave walls was evaluated by a series of kinetic experiments, and partitioning into the liquid phase by the amount of scatter in the data sets.

2.4. Results

A series of variable-time (kinetic) runs was conducted to estimate the amount of time needed for the system to reach equilibrium. These experiments were conducted at 320°C and constant, near-saturated (with liquid) water vapour pressure of about 100 bars, for durations of 1 to 14 days. At this temperature, equilibrium was reached after 6 days, after which *Mo* solubilities were constant to $\pm 28\%$ (Fig. 2). This provides clear evidence that errors due to irreversible

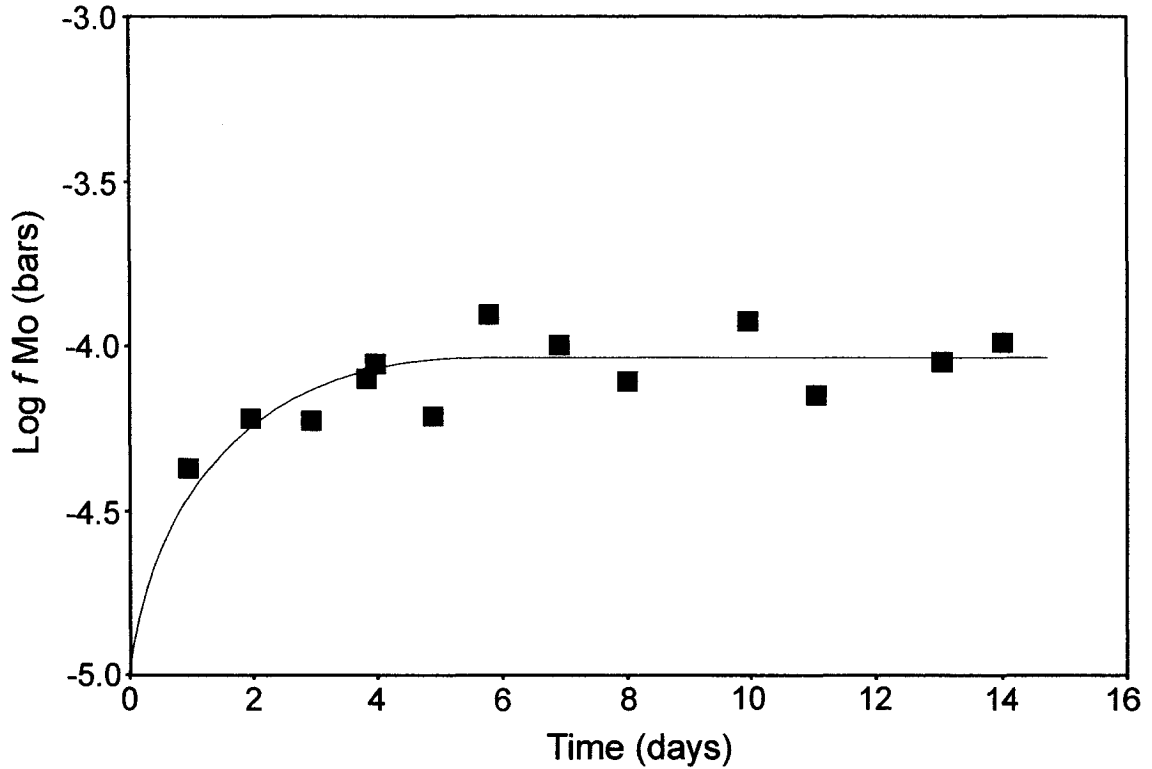


Figure 2: Results of kinetic runs at 320°C, showing the change in molybdenum concentration ($\log f_{\text{MoO}_3 \cdot n\text{H}_2\text{O}}$) with time. Values of $\log f_{\text{MoO}_3 \cdot n\text{H}_2\text{O}}$ are corrected with the Gibbs-Poynting expression, $\frac{V^\circ(P-1)}{RT}$. The solid line is a line of best fit to the experimental data, and indicates that equilibrium was attained after six days. After this time, measured concentrations are within $\pm 28\%$ of the best-fit concentrations.

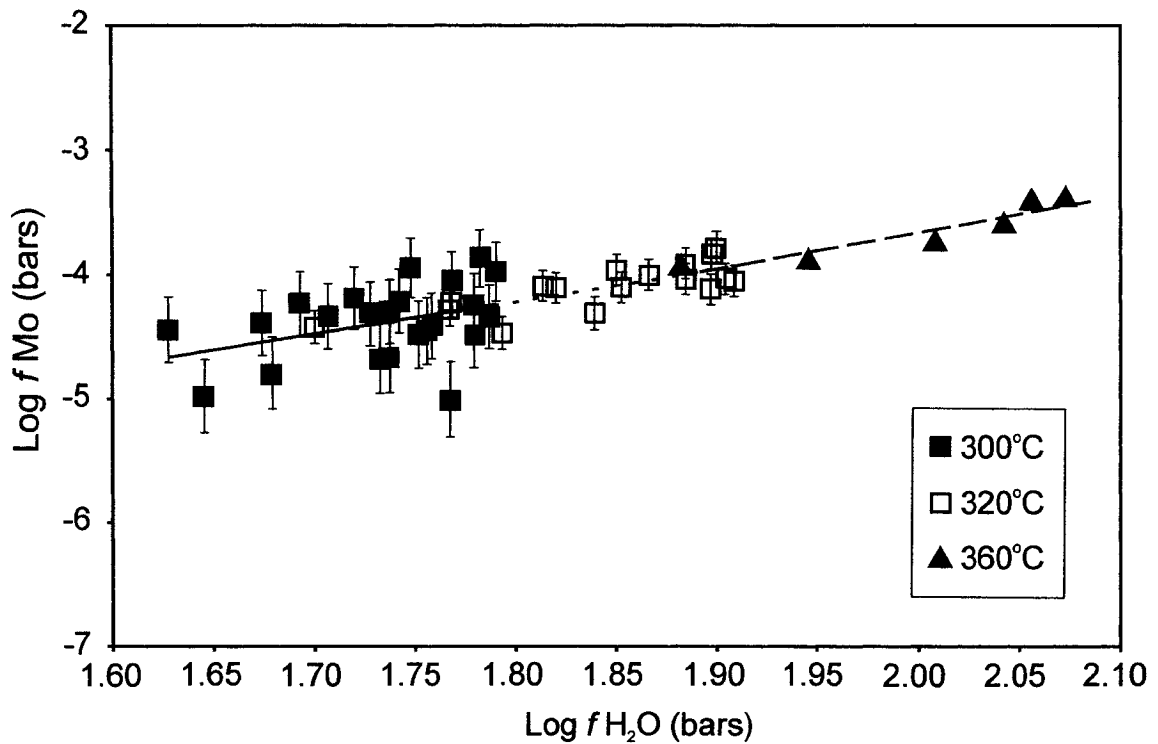


Figure 3: A plot of $\log f_{\text{MoO}_3 \cdot n\text{H}_2\text{O}}$ versus $\log f_{\text{H}_2\text{O}}$ for 300°C, 320°C, and 360°C. Values of $\log f_{\text{MoO}_3 \cdot n\text{H}_2\text{O}}$ are corrected with the Gibbs-Poynting expression, $\frac{V^\circ(P-1)}{RT}$. The data are linearly distributed, and the slope of the best fit line corresponds to the hydration number. The lines of best fit for 300 (solid), 320 (short dash), and 360°C (long dash) are described by the equations $y = 2.6x - 9.0$, $y = 2.5x - 8.0$, and $y = 3.0x - 9.6$, respectively. Hydration numbers, listed in order of increasing temperature, are therefore 2.6, 2.5, and 3.0.

deposition of *Mo* on the walls of the autoclaves and partitioning of *Mo* into the liquid were negligible. All subsequent experiments at 300° and 320°C were conducted for periods of at least 12 days, and those at 360°C for at least 8 days.

Three temperatures (300, 320, and 360°C) were selected at which to investigate the solubility of *Mo* in water vapour. Twenty-three experiments were conducted at 300°C and 48 to 76 bars water vapour pressure (Table 1). At these conditions, the *Mo* concentrations of the run condensates ranged from 1.0 to 13.5 ppm. At 320°C, 13 experiments were conducted, with P_{H_2O} ranging from 57 to 104 bars (Table 2). The run products of these experiments had *Mo* concentrations ranging from 3.2 to 9.5 ppm. The reproducibility of this method, calculated for pairs of experiments run at identical f_{H_2O} , is $\pm 40\%$ at 300°C and $\pm 28\%$ at 320°C. At 360°C, 6 experiments at between 90 and 163 bars were run, resulting in *Mo* concentrations from 9.0 to 23.3 ppm (Table 3). At all three of these temperatures, *Mo* concentrations increased with increasing water vapour pressure, indicating that *Mo* solubility is dependent on the fugacity of water vapour (Fig. 3). Molybdenum solubility, however, does not seem to be dependent on temperature within the range of temperatures investigated, as there was a nearly co-linear correlation of f_{Mo} to f_{H_2O} from 300 to 360°C.

Table 1: Results of experiments measuring the solubility of *Mo* in water vapour at 300°C. H_2O and Mo are the total masses in moles of the corresponding substances introduced into the system (H_2O) and transported in the vapour (Mo). $\text{Log } X_{Mo}$ is the concentration of Mo in the vapour phase expressed as a logarithm of a mole fraction. ϕ_{H_2O} is the fugacity coefficient for H_2O . $\text{Log } f_{H_2O}$ and $\text{log } f_{Mo}$ are the log fugacities of the corresponding gases. GP denotes the Gibbs-

Poynting correction, $\frac{V^o(P-1)}{RT}$.

H_2O , 10^{-1} mol	Mo , 10^{-7} mol	$\text{Log } X_{Mo}$	ϕ_{H_2O}	$\text{Log } f_{H_2O}$, bars	$\text{Log } f_{Mo}$, bars	GP
1.11	1.03	-6.03	0.87	1.67	-4.36	0.034
1.39	0.59	-6.37	0.84	1.73	-4.63	0.041
1.67	1.00	-6.22	0.82	1.78	-4.44	0.047
1.44	1.75	-5.92	0.84	1.74	-4.17	0.042
1.50	0.97	-6.19	0.83	1.75	-4.44	0.043
1.56	1.16	-6.12	0.83	1.76	-4.37	0.044
1.61	2.71	-5.77	0.82	1.77	-4.01	0.045
1.78	0.33	-6.74	0.82	1.77	-4.97	0.045
1.11	0.40	-6.45	0.86	1.68	-4.77	0.035
1.22	1.21	-6.01	0.85	1.71	-4.30	0.038
1.33	0.56	-6.38	0.84	1.73	-4.64	0.041
1.44	1.46	-5.99	0.84	1.74	-4.26	0.041
1.56	1.07	-6.16	0.83	1.76	-4.41	0.044
1.67	1.39	-6.08	0.81	1.79	-4.29	0.048
1.78	3.44	-5.71	0.81	1.79	-3.92	0.048
0.94	0.85	-6.04	0.88	1.63	-4.42	0.030
1.06	0.27	-6.60	0.88	1.65	-4.95	0.032
1.17	1.50	-5.89	0.86	1.69	-4.20	0.036
1.28	1.71	-5.87	0.85	1.72	-4.15	0.039
1.39	1.39	-6.00	0.84	1.73	-4.27	0.040
1.50	3.35	-5.65	0.83	1.75	-3.90	0.042
1.61	1.68	-5.98	0.82	1.78	-4.20	0.047
1.72	4.36	-5.60	0.81	1.78	-3.81	0.048

Table 2: Results of experiments measuring the solubility of *Mo* in water vapour at 320°C. H_2O and Mo are the total masses in moles of the corresponding substances introduced into the system (H_2O) and transported in the vapour (Mo). $\text{Log } X_{Mo}$ is the concentration of Mo in the vapour phase expressed as a logarithm of a mole fraction. ϕ_{H_2O} is the fugacity coefficient for H_2O . $\text{Log } f_{H_2O}$ and $\text{log } f_{Mo}$ are the log fugacities of the corresponding gases. GP denotes the Gibbs-

Poynting correction, $\frac{V^o(P-1)}{RT}$.

H_2O , 10^{-1} mol	Mo , 10^{-7} mol	$\text{Log } X_{Mo}$	ϕ_{H_2O}	$\text{Log } f_{H_2O}$, bars	$\text{Log } f_{Mo}$, bars	GP
2.50	3.33	-5.87	0.72	1.90	-3.97	0.064
2.22	3.07	-5.86	0.79	1.88	-3.98	0.060
1.94	3.33	-5.77	0.81	1.85	-3.92	0.057
1.67	2.31	-5.86	0.83	1.81	-4.05	0.048
1.94	2.42	-5.91	0.81	1.85	-4.05	0.054
2.22	3.95	-5.75	0.79	1.88	-3.87	0.060
1.39	1.36	-6.01	0.85	1.77	-4.24	0.042
1.67	2.17	-5.89	0.83	1.82	-4.07	0.049
1.11	0.91	-6.09	0.88	1.70	-4.39	0.035
1.34	1.53	-5.96	0.85	1.77	-4.19	0.042
1.83	1.45	-6.10	0.82	1.84	-4.26	0.052
2.06	3.10	-5.82	0.80	1.87	-3.95	0.056
1.50	8.95	-6.22	0.84	1.80	-4.43	0.045
2.50	5.35	-5.67	0.78	1.90	-3.77	0.062
2.50	2.82	-5.95	0.78	1.90	-4.05	0.062
2.50	3.16	-5.90	0.77	1.91	-4.00	0.065
2.50	5.86	-5.63	0.77	1.90	-3.73	0.063

Table 3: Results of experiments measuring the solubility of *Mo* in water vapour at 360°C. H_2O and Mo are the total masses in moles of the corresponding substances introduced into the system (H_2O) and transported in the vapour (Mo). $\text{Log } X_{Mo}$ is the concentration of Mo in the vapour phase expressed as a logarithm of a mole fraction. ϕ_{H_2O} is the fugacity coefficient for H_2O . $\text{Log } f_{H_2O}$ and $\text{log } f_{Mo}$ are the log fugacities of the corresponding gases. GP denotes the Gibbs-

Poynting correction, $\frac{V^o(P-1)}{RT}$.

H_2O , 10^{-1} mol	Mo , 10^{-7} mol	$\text{Log } X_{Mo}$	ϕ_{H_2O}	$\text{Log } f_{H_2O}$, bars	$\text{Log } f_{Mo}$, bars	GP
1.67	2.92	-5.76	0.85	1.88	-3.87	0.051
2.22	3.76	-5.77	0.82	1.94	-3.83	0.062
2.78	5.94	-5.67	0.78	2.01	-3.66	0.075
3.33	9.38	-5.55	0.75	2.04	-3.51	0.084
3.89	16.34	-5.38	0.74	2.06	-3.32	0.089
4.44	19.43	-5.36	0.72	2.07	-3.29	0.094

2.5. Discussion

2.5.1. Data treatment

As experimentally-determined *Mo* fugacities are roughly twenty orders of magnitude higher than in the water-free system (10^{-24} bars at 320°C, calculated using data from Pankratz, 1982; Figure 4), it is evident that the solvent plays an important role in *Mo* solubility. The observed increase in f_{Mo} with f_{H_2O} (Fig. 3) indicates that the gaseous speciation of *Mo* is dependent on water fugacity. This dependence of molybdenum solubility on f_{H_2O} indicates that the metal forms a gaseous hydrated complex of the form $MoO_3 \cdot nH_2O$ by the reaction:



In the calculations that follow, it is assumed that the partial pressure of MoO_3 is negligible compared to that of H_2O , and thus the total vapour pressure of the system is equal to the partial pressure of water vapour. Water fugacities were calculated using the equation of state of Kestin *et al.* (1984), whereas the fugacity of the gaseous *Mo* hydrate was calculated using the *Mo* concentrations of the run products. The mole fraction of *Mo* is therefore given by

$$X_{MoO_3 \cdot nH_2O} \cong \frac{M_{MoO_3 \cdot nH_2O}}{M_{H_2O}}, \quad (2)$$

where M is the number of moles of the corresponding component. As fugacity coefficients for the gaseous *Mo* hydrate are unknown, the species was treated as an ideal gas, and thus

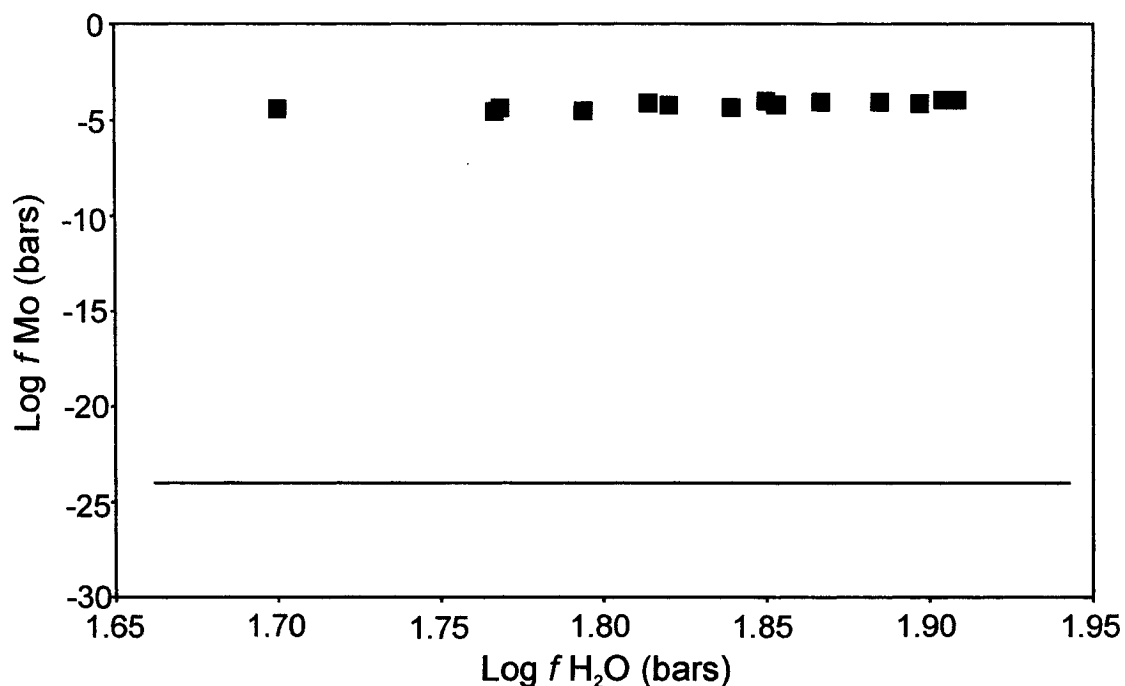
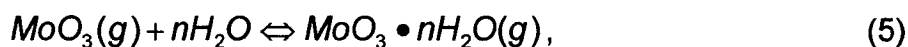


Figure 4: A plot of $\log f_{MoO_3 \cdot nH_2O}$ versus $\log f_{H_2O}$ for dry and wet systems at 320°C. Values of $\log f_{MoO_3 \cdot nH_2O}$ are corrected with the Gibbs-Poynting expression, $\frac{V^\circ(P-1)}{RT}$. Closed squares are experimentally-determined data points, and the solid line is the fugacity of MoO_3 in a water-free system. The data show that the fugacity of MoO_3 is roughly twenty orders of magnitude higher in the presence of water.

$$X_{\text{MoO}_3 \cdot n\text{H}_2\text{O}} \cong \frac{f_{\text{MoO}_3 \cdot n\text{H}_2\text{O}}}{f_{\text{H}_2\text{O}}} \quad (3)$$

As discussed in Migdisov *et al.* (1999), the hydration number (n) for the product of reaction (1) can be determined from the differentiation of the expression for the logarithm of the equilibrium constant ($\log K$), as discussed below. However, as the formation of the hydrated complex involves both $\text{MoO}_3(s)$ and $\text{MoO}_3(g)$, $\log K$ is dependent on the total pressure of the system ($P_{\text{total}} \approx P_{\text{H}_2\text{O}}$). In order to convert this heterogeneous system into one that is independent of pressure, reaction (1) was considered to represent the following two consecutive reactions:



where the latter expression is a homogeneous gas-phase reaction, and is therefore independent of pressure for ideal gases. The equilibrium constant for equation (4) is dependent on the total pressure of the system as follows:

$$\frac{d \log K_4}{d \log P_{\text{total}}} = \int_{P_1}^{P_2} \frac{V^\circ}{RT} dP \cong \frac{V^\circ(P_1 - P_2)}{RT}, \quad (6)$$

where V° is the molar volume of $\text{MoO}_3(s)$ (3.056 J bar^{-1} ; Robie *et al.*, 1966), and

$\frac{V^\circ(P-1)}{RT}$ is the Poynting correction (Sandler, 1989). The fugacity of gaseous

molybdenum trioxide must thus be corrected as follows:

$$\log f_{\text{MoO}_3(P,T)} = \log f_{\text{MoO}_3(P=1,T)} + \frac{V^\circ(P-1)}{RT}, \quad (7)$$

where f_{MoO_3} is constant at constant pressure. The equilibrium constant for reaction (5) is thus given by the following expression:

$$\begin{aligned} \log K_5 &= \log f_{MoO_3 \cdot nH_2O} - n \log f_{H_2O} - \log f_{MoO_{3(P,T)}} \\ &= \left(\log f_{MoO_3 \cdot nH_2O} - \frac{V^\circ(P-1)}{RT} \right) - n \log f_{H_2O} - \log f_{MoO_{3(P=1,T)}} \end{aligned} \quad (8)$$

Differentiation of this expression with respect to f_{H_2O} at constant temperature gives:

$$\left(\frac{\partial \left(\log f_{MoO_3 \cdot nH_2O} - \frac{V^\circ(P-1)}{RT} \right)}{\partial \log f_{H_2O}} \right)_T = n \quad (9)$$

From equation 9, it follows that the hydration number n can be derived from the slope of a line representing a plot of the experimentally-determined values of $\log f_{MoO_3 \cdot nH_2O} - \frac{V^\circ(P-1)}{RT}$ versus $\log f_{H_2O}$ (Fig. 3). The hydration number so determined was approximately 2.6 at 300°C, 2.5 at 320°C, and 3.0 at 360°C. Equilibrium constants for reaction (5) were calculated for each isotherm using experimentally-determined fugacities of $MoO_3 \cdot nH_2O$ and H_2O , and equaled 16.9, 16.5, and 12.5 for 300, 320, and 360°C, respectively.

2.5.2. Oxidation state of molybdenum

Molybdenum commonly speciates as $Mo(IV)$ and $Mo(VI)$, but the fugacity of $Mo(VI)$ trioxide in a dry system is roughly 15 orders of magnitude greater than $Mo(IV)$ dioxide (calculated using data from Pankratz, 1982), and thus hydrated

Mo(VI) trioxide is likely the predominant gaseous species in water vapour. To test this hypothesis, two experimental runs at 320°C and near-saturated water vapour pressure were held at a constant oxidation state with a MoO_2 - MoO_3 buffer. Separate sample ampoules and holders were used for MoO_2 and MoO_3 , and care was taken to ensure that no pre-run cross-contamination occurred between the two. The Mo concentrations of the condensed water from these runs were identical to those of the non-buffered runs at 320°C (Fig. 5), confirming that the predominant gaseous Mo species at the conditions of the experiments was a molybdenum(VI) trioxide hydrate. Post-run XRD analysis of the MoO_2 and MoO_3 ampoules showed that while no MoO_3 was reduced to MoO_2 , MoO_2 was partially oxidized to MoO_3 , indicating that the excess oxygen in the system was consumed. The oxygen fugacity was thus effectively buffered at the MoO_2 - MoO_3 boundary (1×10^{-22} bars).

2.5.3. Stability of hydrated species

A hydration (solvation) number of 2 – 3 indicates that Mo forms a di- to tri-hydrate in the vapour phase ($MoO_3 \cdot 2-3H_2O$). This coordination is possible, as MoO_3 and its hydrates are known to have octahedral structure. For example, an XRD study by Krebs (1972) showed that Mo in the crystal structure of $MoO_3 \cdot 2H_2O$ is coordinated to five oxygen atoms and one molecule of H_2O , which form a distorted octahedron around Mo. In this example, the second water molecule acts as hydrate water between the layers of octahedra, and is not coordinated to Mo. Molybdenum is also octahedrally-coordinated in α - $MoO_3 \cdot H_2O$, where it forms

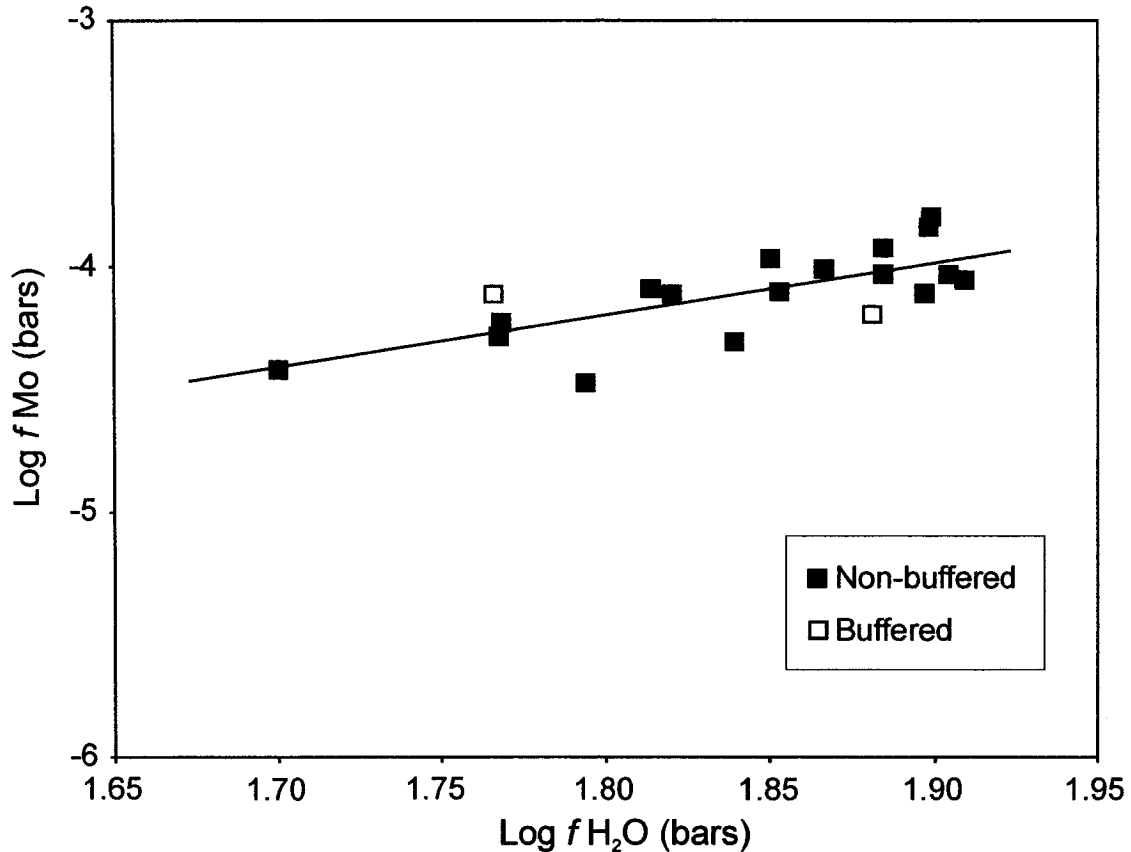


Figure 5: A plot of $\log f_{MoO_3 \cdot nH_2O}$ versus $\log f_{H_2O}$ for buffered and non-buffered experiments at 320°C. Values of $\log f_{MoO_3 \cdot nH_2O}$ are corrected with the Gibbs-Poynting expression, $\frac{V^\circ(P-1)}{RT}$. When buffered data are added to the plot, the equation of the line of best fit changes from $y = 2.5x - 8.0$ to $y = 2.1x - 8.0$. The data from buffered runs are co-linear to those from non-buffered experiments, indicating that the reaction $MoO_3(g) + nH_2O \rightleftharpoons MoO_3 \cdot nH_2O(g)$ is independent of oxygen fugacity, i.e., that the dominant gaseous *Mo* species at the conditions of the experiment contains *Mo(VI)* rather than *Mo* in any other oxidation state.

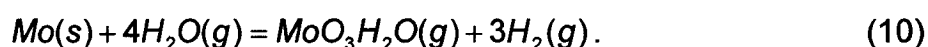
double chains of edge-sharing $[MoO_5(H_2O)]$ octahedra (Boeschen and Krebs, 1974). In aqueous solution (liquid), where the behaviour of *Mo* may be similar to that in the gaseous state, the metal is also known to form octahedral complexes. EXAFS and XANES analyses by Yokoi *et al.* (1993) showed that in <3M *HCl* solutions, *Mo* exists as hydrates such as $MoO_2(H_2O)_4^{2+}$, where the central *Mo* atom is coordinated octahedrally. Similarly, Ozeki *et al.* (1996) examined the dissolved structures of MoO_4^{2-} , $HMoO_4^+$, and H_2MoO_4 with UV-visible spectroscopy, and determined that, while the former two species exist in aqueous solution as tetrahedral complexes, the third species is a distorted octahedron. Finally, Messaoudi *et al.* (2004) used density function calculations to examine the dimerization of $MoO_2(OH)(H_2O)_3^+$ to form $Mo_2O_5(H_2O)_6^{2+}$ in both the gas and liquid phases, and determined that the reactant species is most stable as an octahedron defined by the three H_2O ligands.

Measured molybdenum solubilities indicate that the formation of hydrated complexes increases the volatility of the metal by up to twenty orders of magnitude. The fugacity of $MoO_3(g)$ in a water-free system, calculated using data from Pankratz (1982), is on the order of 10^{-24} bars at 320°C (Fig. 4). In comparison, experimentally-determined fugacities of $MoO_3 \cdot nH_2O$ are approximately 10^{-4} bars. These greatly increased *Mo* solubilities indicate clearly that solvent-solute interactions govern the solubility of MoO_3 in water vapour.

2.5.4. Comparison with other studies

Early experimental studies suggested that *Mo* forms hydrated complexes in aqueous vapour, and that the formation of these complexes causes an appreciable increase in *Mo* solubility. From measurements of the mass of *Mo* trioxide precipitated from a stream of water vapour at 600-700°C, Millner and Neugebauer (1949) concluded that the volatility of MoO_3 increases with P_{H_2O} and temperature, and suggested that *Mo* dissolves as $MoO_3 \cdot H_2O(g)$. Elliot (1952) and Sardi (1963) observed a similar dependence between 550-560°C and 580-730°C, respectively, and came to the same conclusion regarding speciation. However, as Millner and Neugebauer (1949) and Elliot (1952) reported only four and three data points, respectively, and as the experiments of Sardi (1963) did not attain equilibrium, the stoichiometry of the dissolved complex was not established.

Belton and Jordan (1965), using a weight-loss method, later determined the stoichiometry of the *Mo* monohydrate at temperatures from 1200 to 1500°C and water vapour pressures from 0.04 to 0.5 bars. These researchers observed an increase in the apparent vapour pressure of *Mo* with P_{H_2O} (Fig. 6), and used a ratio of water vapour to pure hydrogen gas to calculate the number of oxygen atoms in the *Mo* species, based on the reaction:



The apparent vapour pressures of this complex at the conditions of the experiments were between 1.67×10^{-5} and 133.80×10^{-5} bars, increasing with

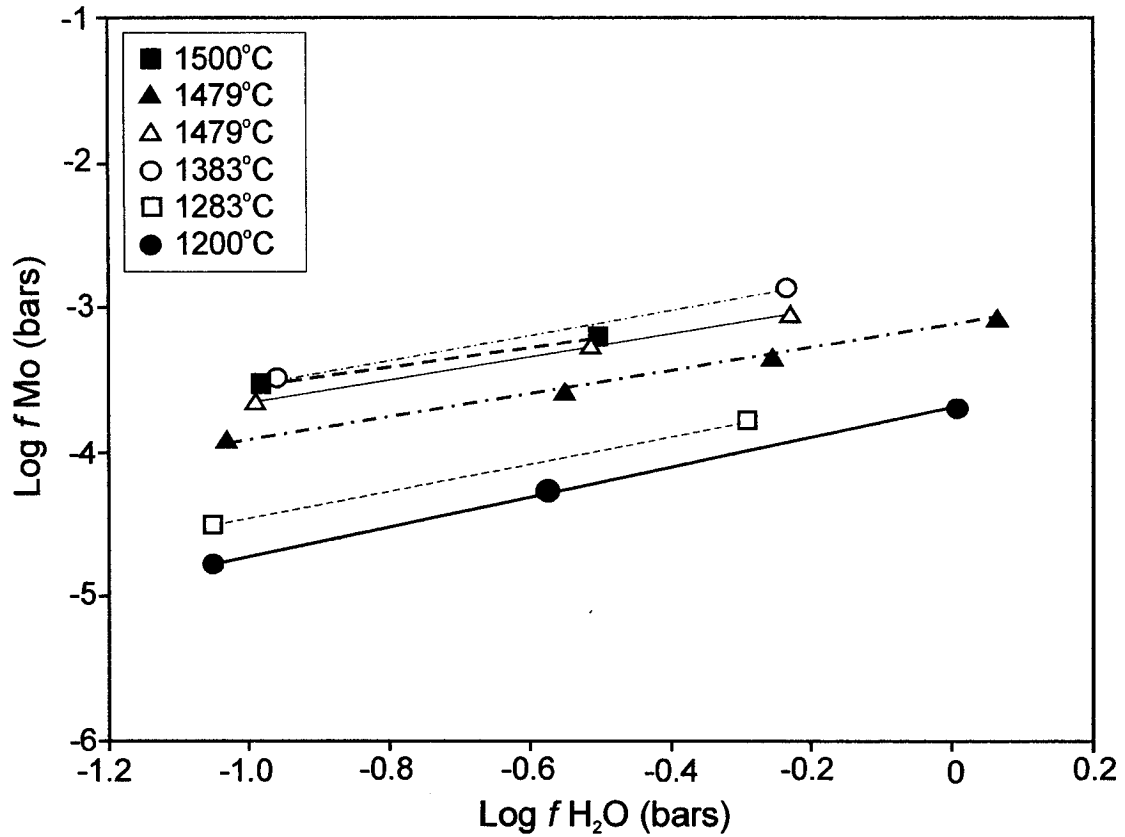


Figure 6: A plot of $\log f_{Mo}$ versus $\log f_{H_2O}$ at 1200-1500 °C, from Belton and Jordan (1963). Solid triangles represent experiments carried out with $H_2O/H_2=0.82$ and open circles represent those with $H_2O/H_2=1.40$. All other experiments had $H_2O/H_2=1.00$. The hydration numbers of the gaseous Mo complexes are given by the slope of the lines of best fit, and are as follows: 0.9995 for 1200°C, 0.9466 for 1283°C, 0.8708 for 1383°C, 0.8005 for 1479°C (open triangles), 0.7661 for 1479°C (closed triangles), and 0.6862 for 1500°C.

temperature. These authors also interpreted the gaseous *Mo* species as $MoO_3 \cdot H_2O$, although their data, presented in figure 6, show a variation in hydration number with temperature.

Results of experiments conducted in the present study support the conclusions of previous experimental studies, namely that MoO_3 dissolves as a hydrate in water vapour. However, previous interpretations of the species as a monohydrate are at odds with the results presented here, which indicate a hydration number of >2 . The likely explanation for this, which is suggested by studies of other systems, is that the hydration number of the gaseous species decreases with increasing temperature. For example, Archibald *et al.* (2001, 2002) determined that the hydration number of gold-chlorine species decreases from 5 at 300°C to 3 at 360°C, and that of gaseous copper chloride species decreases from 7.6 at 320°C, to 6.0 at 300°C, to 6.1 at 280°C. Similarly, Migdisov and Williams-Jones (*submitted*) found that the hydration number of gaseous tin oxychloride species decreased from 2.9 to 2.5 with a temperature increase from 300 to 350°C, respectively.

In order to evaluate the possible effect of temperature on hydration number, the data collected in the present study were compared with those from Belton and Jordan (1963). As shown in Figure 7, the hydration number increases linearly from high temperature (data from Belton and Jordan, 1963) to low temperature (this study). This observation supports the interpretation that the gaseous *Mo*

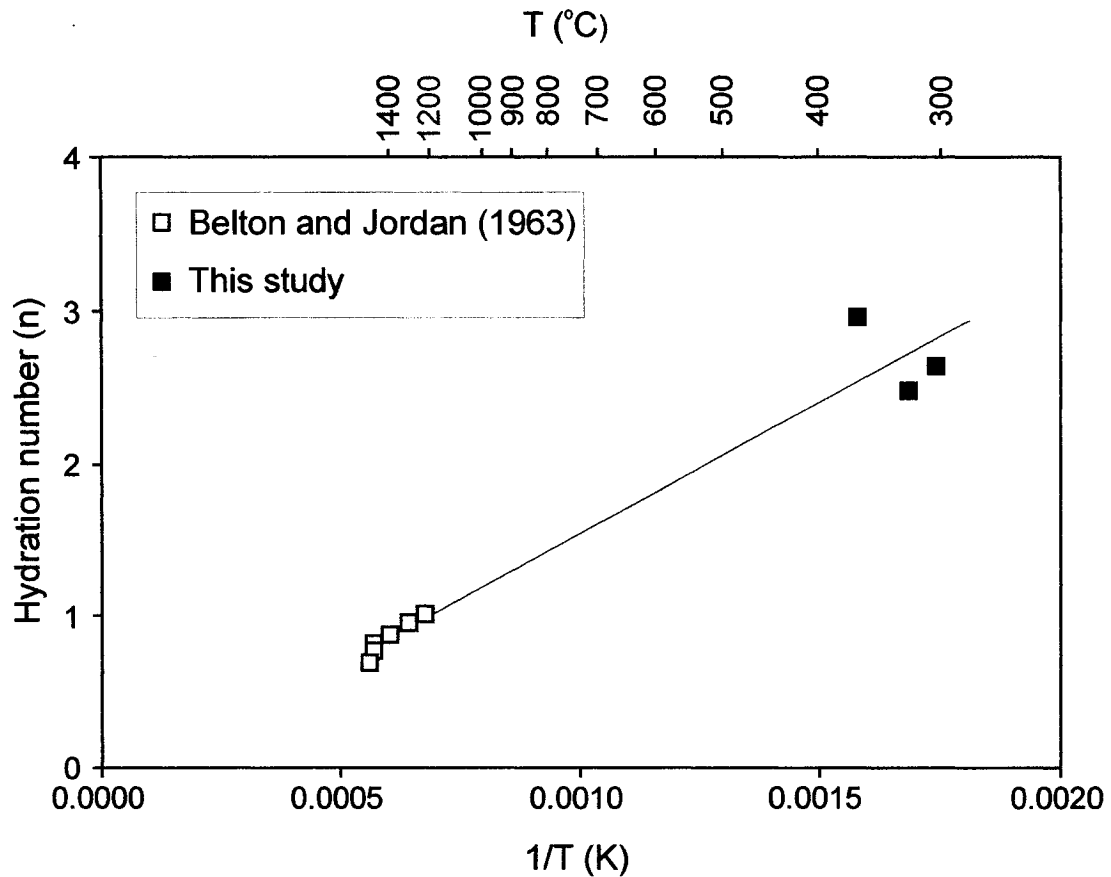


Figure 7: A plot of hydration number (n) versus reciprocal temperature. Open squares represent data from Belton and Jordan (1963), and closed squares represent data collected in the present study. The solid line is the line of best fit through both data sets, and shows that the hydration number (n) decreases with increasing temperature.

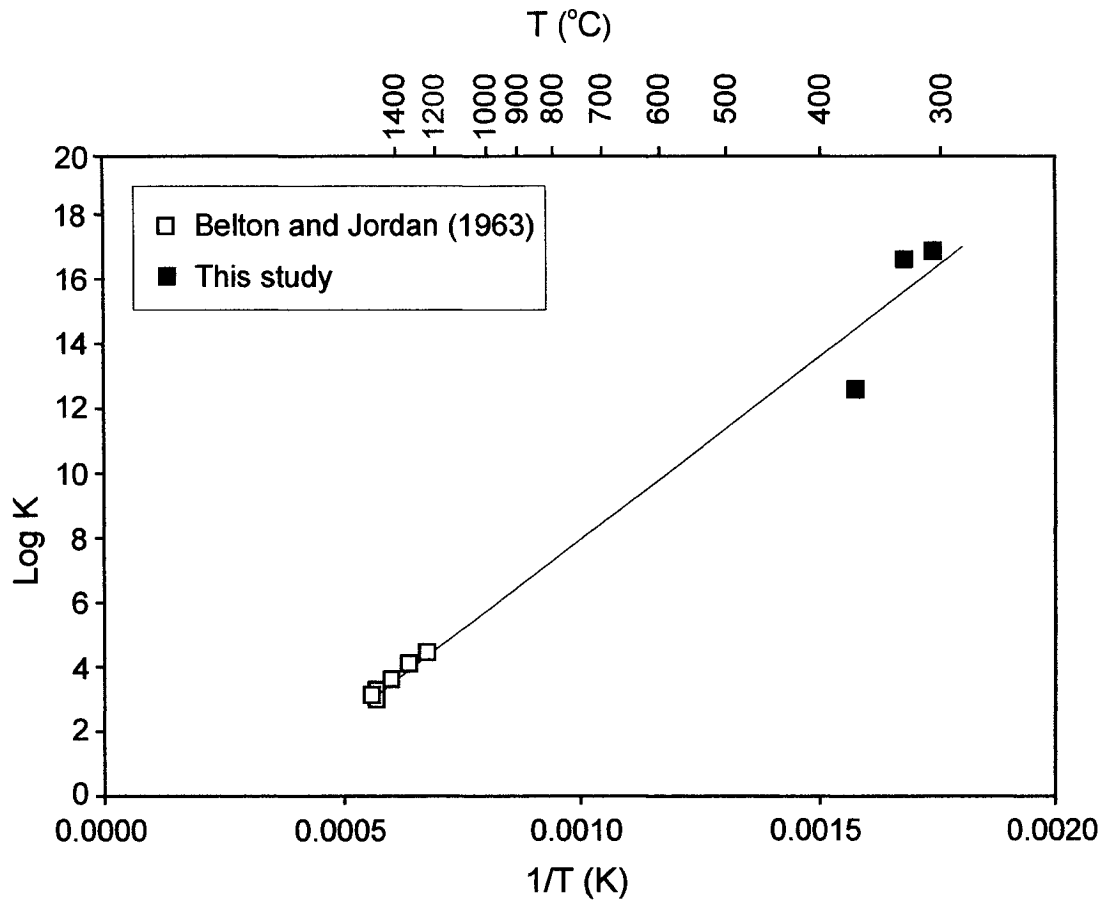


Figure 8: A plot of the logarithm of the equilibrium constant for the reaction $\text{MoO}_3(g) + n\text{H}_2\text{O} \rightleftharpoons \text{MoO}_3 \cdot n\text{H}_2\text{O}(g)$ versus reciprocal temperature. Open squares represent values of $\log K$ calculated from data in Belton and Jordan (1963), and closed squares represent values of $\log K$ from the present study. The solid line represents the line of best fit through both data sets, and indicates that the stability of the hydrated species increases with decreasing temperature.

species is a hydrated complex, and indicates that the hydration shell gradually breaks down with increasing temperature.

Similarly, values of $\log K$ for reaction (5) increase with decreasing temperature. The equilibrium constants determined in the present study, when plotted versus reciprocal temperature (Fig. 8), are co-linear with those calculated from data of Belton and Jordan (1963). The increase in $\log K$ with decreasing temperature corresponds to a decrease in Gibbs free energy, indicating that the formation of the hydrated complex is favoured by decreasing temperature.

2.5.5. Geological implications

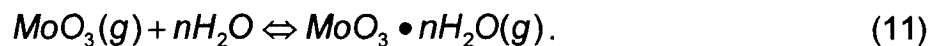
The *Mo* concentrations observed in the run condensates were many orders of magnitude higher than those predicted thermodynamically for the water-free system. For example, Krauskopf (1957, 1964) found that the volatility of $MoO_3(g)$, the *Mo* species thought to dominate magmatic vapour, was about 30 ppm in water vapour at 827°C, but decreased dramatically with decreasing temperature and oxygen fugacity. The high *Mo* solubility at low temperature observed in the present study indicates that the vapour phase may play a much more important role in the transport of *Mo* in natural systems than previously thought. For example, as the vapour phase is thought to dominate porphyry-forming systems (Henley and McNabb, 1978), vapour transport may be an important process in the formation of economic *Mo* porphyry deposits.

If the measured *Mo* solubility data are extrapolated to 600°C, a typical temperature for a porphyry system (White *et al.*, 1981), and *Mo* concentrations are calculated to be in equilibrium with molybdenite, the primary *Mo* ore mineral, with f_{O_2} and f_{S_2} controlled by the assemblage hematite-magnetite-pyrite, (using data from Pankratz, 1982 and Pankratz *et al.*, 1987), a solubility of 0.06 ppm *Mo* is obtained (see Appendix for calculations). Assuming a water vapour flux of 5 million tonnes per year (measured at actively degassing fumaroles from Satsuma-Iwojima volcano, Japan), and sufficient reduced sulphur to take up all of the *Mo*, approximately 0.32 tonnes *Mo* can feasibly be transported and deposited annually. The formation of a high-grade *Mo* porphyry deposit, such as the Endako porphyry, British Columbia (336 Mt at 0.087% *Mo*), would therefore take about 900,000 years, which is within the lifetime of some known geothermal systems (Silberman and White, 1975; Christiansen, 1984). In light of this calculation, a reassessment of current models for porphyry *Mo* deposits may be necessary.

2.6. Conclusions

It has been shown experimentally that economically significant amounts of MoO_3 can potentially be transported in water vapour, and that the solubility of MoO_3 is approximately 20 orders of magnitude higher than that predicted for the water-free system. It was also observed that the solubility of MoO_3 increases with increasing water fugacity. This dependence of molybdenum solubility on f_{H_2O}

indicates that the metal forms a gaseous hydrated complex of the type $MoO_3 \cdot nH_2O$ by the reaction:



When compared to high-temperature data collected by Belton and Jordan (1963), the hydration number, n , appears to decrease with increasing temperature. A hydration number of 2.6 was obtained at 300°C, 2.5 at 320°C, and 3.0 at 360°C (this variation in hydration number over the small temperature range of the experiments is probably an artifact and therefore not significant). When compared with published data on the solubility of MoO_3 at higher temperatures, a decrease in hydration number with increasing temperature is evident (n decreased from 1.0 to 0.69 with a temperature increase from 1200 to 1500°C; Belton and Jordan, 1963). Likewise, equilibrium constants for reaction (11) decrease with increasing temperature; $\log K$ is equal to 16.9 at 300°C, 16.5 at 320°C and 12.5 at 360°C. Logarithms of equilibrium constants calculated from published data at higher temperatures decrease from 3.7 to 2.8 with a temperature increase from 1200 to 1500°C.

Calculations based on physicochemical conditions typical of porphyry molybdenum systems indicate that MoO_3 is sufficiently soluble in water vapour as a hydrated complex to allow the formation of a porphyry Mo deposit of economic grade, by vapour transport alone, within the lifetime of a geothermal system.

2.7. References

- Archibald, S.M., Migdisov, A.A. and Williams-Jones, A.E. (2001) The stability of Au-chloride complexes in water vapor at elevated temperatures and pressures. *Geochim. Cosmochim. Acta* 65: 4413-4423.
- Archibald, S.M., Migdisov, A.A. and Williams-Jones, A.E. (2002) An experimental study of the stability of copper chloride complexes in water vapor at elevated temperatures and pressures. *Geochim. Cosmochim. Acta* 66: 1611-1619.
- Belton, G.R. and Jordan, A.S. (1965) The volatilization of molybdenum in the presence of water vapor. *J. Phys. Chem.* 69: 2065-2071.
- Boeschen, I. and Krebs, B. (1974) Crystal structure of white molybdic acid, α - $\text{MoO}_3 \cdot \text{H}_2\text{O}$. *Acta Cryst.* 30: 1795-800.
- Burnham, C.W. (1979) Magmas and hydrothermal fluids. In: *Geochemistry of Hydrothermal Ore Deposits*, 2nd Edition. Ed: H.L. Barnes. John Wiley & Sons, Toronto, 798 pp.
- Christiansen, R.L. (1984) Yellowstone magmatic evolution: its bearing on understanding large-volume explosive volcanism. In: *Studies in Geophysics: Explosive Volcanism: Inception, Evolution, and Hazards*. National Academic Press, Washington, D.C., pp. 84-95.
- Eastoe, C.J. (1982) Physics and chemistry of the hydrothermal system at the Pangua porphyry deposit, Bougainville, Papua New Guinea. *Econ. Geol.* 77, 127-153.

- Elliot, R.B. (1952) Gaseous hydrated oxides, hydroxides, and other hydrated molecules. *University of California, Radiation Laboratory Report 1831*, 52 pp.
- Heinrich, C.A., Ryan, C.G., Mernagh, T.P. and Eadington, P.J. (1992) Segregation of ore metals between magmatic brine and vapor: a fluid inclusion study using PIXE Microanalysis. *Econ. Geol.* 87: 1566-1583.
- Heinrich, C.A., Günther, D., Audétat, A., Ulrich, T. and Frischknecht, R. (1999) Metal fractionation between magmatic brine and vapor, determined by microanalysis of fluid inclusions. *Geology* 27: 755-758.
- Henley, R.W. and McNabb, A. (1978) Magmatic vapor plumes and ground-water interaction in porphyry copper emplacement. *Econ. Geol.* 73: 1-19.
- Kestin, J., Sengers, J.V., Kamgar-Parsi, B. and Levelt Sengers, J.M.H. (1984) Thermophysical properties of fluid water. *J. Phys. Chem. Ref. Data* 13: 175-183.
- Krauskopf, K.B. (1957) The heavy metal content of magmatic vapor at 600°C. *Econ. Geol.* 52: 786-807.
- Krauskopf, K.B. (1964) The possible role of volatile metal compounds in ore genesis. *Econ. Geol.* 59: 22-45.
- Krebs, B. (1972) Crystal structure of molybdenum trioxide dihydrate. *Acta Cryst.* 28: 2222-2231.
- Messaoudi, S., Furet, E., Gautier, R., Le Fur, E. and Pivan, J.-Y. (2004) A density functional study of the dimerization mechanisms of molybdenum(vi) in aqueous solution. *Phys. Chem.* 6, 2083-2087.

- Migdisov, A.A., Williams-Jones, A.E. and Suleimenov, O.M. (1999) Solubility of chlorargyrite (AgCl) in water vapor at elevated temperatures and pressures. *Geochim. Cosmochim. Acta* 63: 3817-3827.
- Migdisov, A.A. and Williams-Jones, A.E. An experimental study of cassiterite solubility in HCl-bearing water vapor. (*submitted.*)
- Millner, T. and Neugenbauer, J. (1949) Volatility of the oxides of tungsten and molybdenum in the presence of water vapour. *Nature* 163: 601-602.
- Ozeki, T., Adachi, H. and Ikeda, S. (1996) Estimation of the dissolved structures and condensation reactivities of mononuclear molybdenum(VI) species in solution using UV-vis absorption spectra and molecular orbital calculation DV-X α . *Bull. Chem. Soc. Japan* 69: 619-625.
- Pankratz, L.B. (1982) *Thermodynamic Properties of Elements and Oxides*. United States Bureau of Mines, Bulletin 672, 509 pp.
- Pankratz, L.B., Mah, A.D. and Watson, S.W. (1987) *Thermodynamic Properties of Sulfides*. United States Bureau of Mines, Bulletin 689, 427 pp.
- Reynolds, T.J. and Beane, R.E. (1985) Evolution of hydrothermal fluid characteristics at the Santa Rita, New Mexico porphyry deposit. *Econ. Geol.* 80: 1328-1347.
- Robie, R.A., Bethke, P.M., Toulmin, M.S. and Edwards, J.L. (1966) X-ray crystallography data, densities, and molar volumes of minerals. In: *Handbook of Physical Constants*, revised edition. Ed: S.P. Clark. GSA memoir 97, pp. 437-458.

- Sandler, S.I. (1989) *Chemical and Engineering Thermodynamics*. John Wiley and Sons, New York, 622 pp.
- Sardi, A. (1963) Reduction of Mo trioxide II. Appearance of oxides phases between Mo trioxide and Mo dioxide during reduction of Mo trioxide by a flowing gas mixture containing H and water. *Acta Chim. Acad. Sci. Hung.* 39: 145-160.
- Silberman, M.L. and White, D.E. (1975) Limits on duration of hydrothermal activity at Steamboat Springs, Nevada, by K-Ar ages of spatially distributed associated altered and unaltered volcanic rocks. *Econ. Geol.* 70: 1329.
- Symonds, R.B., Rose, W.I., Reed, M.H., Lichte, F.E. and Finnegan, D.L. (1987) Volatilization, transport, and sublimation of metallic and non-metallic elements in high temperature gases at Merapi Volcano, Indonesia. *Geochim. Cosmochim. Acta* 51: 2083-2101.
- Ulrich, T., Gunther, D. and Heinrich, C.A. (1999) Gold concentrations of magmatic brines and the metal budget of porphyry copper deposits. *Nature* 399: 676-679.
- White, W.H., Bookstrom, A.A., Kamilli, R.J., Ganster, M.W., Smith, R.P., Ranta, D.E. and Steininger, R.C. (1981) Character and origin of Climax-type molybdenum deposits. *Econ. Geol.* 75th Anniversary Volume: 270-316.
- Williams-Jones, A.E., Migdisov, A.A., Archibald, S.M. and Xiao, Z. (2002) Vapor-transport of ore metals. In: *Water-Rock Interaction, Ore Deposits, and Environmental Geochemistry: A Tribute to David A. Crerar*. Eds: R.

Hellmann and S.A. Wood. The Geochemical Society, Special Publication No. 7, pp. 279-305.

Yokoi, K., Matsubayashi, N., Miyanaga, T., Watanabe, I. and Ikeda, S. (1993) Studies on the structure of molybdenum(VI) in acidic solution by XANES and EXAFS. *Polyhedron* 12: 911-914.

CHAPTER 3

EXTENDED CONCLUSIONS

Conclusions

In the preceding chapter, an experimental investigation of the solubility of molybdenum in water vapour was reported. The conclusions of this research are as follows:

- (1) The solubility of *Mo* in water vapour is 20 orders of magnitude higher than that in a water-free system. This indicates that water vapour plays an important role in gaseous *Mo* speciation, and that the role of water vapour in the transport of *Mo* is significantly greater than previously thought.
- (2) Over the temperature range of 300-360°C, *Mo* solubility increases from 1.3 to 23.3 ppm with an increase in water fugacity from 48 to 163 bars. The correlation between solubility and water fugacity indicates that molybdenum forms a hydrated gaseous complex of the type $MoO_3 \cdot nH_2O$, where *n* is the hydration number.
- (3) On a plot of $\log f_{H_2O}$ versus $\log f_{Mo}$, the hydration number, *n*, is given by the slope of the line of best fit. The hydration number is 2.6 at 300°C, 2.5 at 320°C, and 3.0 at 360°C, which indicates that the gaseous molybdenum hydrate is $MoO_3 \cdot 2-3H_2O$.

- (4) When compared with published data for the solubility of molybdenum in water vapour at 1200-1500°C, a decrease in hydration number with increasing temperature is evident. This observation implies that the hydration shell begins to break down with increasing temperature.
- (5) The logarithm of the equilibrium constant, $\log K$, for the reaction $MoO_3(g) + nH_2O(g) = MoO_3 \cdot nH_2O(g)$ is 16.9 at 300°C, 16.5 at 320°C, and 12.5 at 360°C. This decrease in $\log K$ with increasing temperature demonstrates that the hydrated complex is less stable at higher temperatures.
- (6) A model of a simplified *Mo* porphyry-forming system, using *Mo* solubilities calculated in equilibrium with molybdenite and extrapolated to 600°C and 500 bars, average water vapour and total sulphur fluxes from an actively degassing volcano, and f_{O_2} and f_{S_2} controlled by the assemblage hematite-magnetite-pyrite, demonstrates that the vapour phase can transport sufficient *Mo*, within the lifetime of a geothermal system, to produce an economic *Mo* porphyry deposit (e.g., the Endako deposit, BC, with 336 Mt at 0.087% *Mo*).

Recommendations for future research

The *Mo*-*H*₂*O* fluid modeled in these experiments is an extremely simplified ore-forming system. In order to better represent the solubility of *Mo* in

porphyry-forming fluids, this system should be extended with the addition of other components. While H_2O may be a dominant ligand in the formation of gaseous *Mo* species, other components such as *HF* or *HCl* may also serve to increase molybdenum solubility. Of these two components, *HF* may be the most important, as *F* is a relatively hard ion and often associated with *Mo* in porphyry deposits (White *et al.* 1981), and is known to form a number of stable gaseous *Mo* species (Hildenbrand, 1976). Chlorine may also be very important, as it is a major constituent in ore-forming fluids and is known to speciate with molybdenum in aqueous solutions and vapours (e.g., Hultgren and Brewer, 1956; Cannon, 1959).

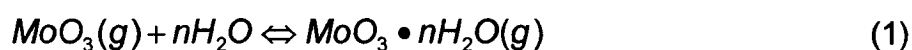
Future work investigating the partitioning of molybdenum between aqueous liquid and vapour at the conditions of a porphyry system would also be very important, as this would give a clear indication of the true role of water vapour in the formation of *Mo* porphyry deposits. If, as Ulrich *et al.* (1999) observed at Grasberg, Indonesia, *Mo* partitions preferentially into the liquid phase, the vapour transport of *Mo* may not be a dominant process. On the other hand, if *Mo* partitions preferentially into the aqueous vapour (as seen at Bajo de la Alumbrera, Argentina; Ulrich *et al.*, 1999), then the vapour plays a much more important role in the formation of *Mo* ore deposits than previously thought, and modification of the current models of porphyry *Mo* deposit formation will be necessary.

References

- Cannon, P. (1959) The solubility of molybdenum trioxide in various mineral acids. *J. Inorg. Nucl. Chem.* 11: 124-127.
- Hildenbrand, D.L. (1976) Thermochemical studies of the gaseous lower-valent fluorides of molybdenum. *J. Chem. Phys.* 65: 614-618.
- Hultgren, N., Brewer, L. (1956) Gaseous molybdenum oxychloride. *J. Phys. Chem.* 60: 947-949.
- Ulrich, T., Gunther, D. and Heinrich, C.A. (1999) Gold concentrations of magmatic brines and the metal budget of porphyry copper deposits. *Nature* 399: 676-679.
- White, W.H., Bookstrom, A.A., Kamilli, R.J., Ganster, M.W., Smith, R.P., Ranta, D.E. and Steininger, R.C. (1981) Character and origin of Climax-type molybdenum deposits. *Econ. Geol.* 75th Anniversary Volume: 270-316.

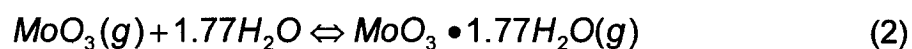
Appendix: Extrapolation of experimental data to 600°C

In order to estimate the solubility of *Mo* in water vapour at 600°C (a typical temperature for *Mo*-porphyry ore-forming systems), the experimental data collected at 300, 320, and 360°C were extrapolated using high-temperature (1200-1500°C) data collected by Belton and Jordan (1963). A comparison of high- and low-temperature data shows that the logarithm of the equilibrium constant ($\log K$) for the reaction



decreases with increasing temperature (Fig. 8). $\log K$ for 600°C was therefore taken from the line of best fit between the two data sets on a graph of $\log K$ versus inverse temperature ($1/T$, K; Fig. 8). Likewise, as the hydration number, n , decreased with increasing temperature, n for 600°C was taken from the line of best fit between high and low temperature data on a plot of n vs. $1/T$ (K; Fig. 7). Solving the equations of the lines of best fit for 600°C gave a $\log K$ equal to 9.54 and a hydration number of 1.77.

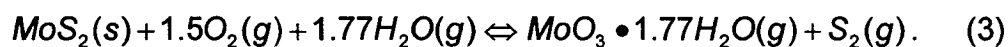
The Gibbs free energy of reaction ($\Delta_r G$) for:



was then calculated directly from the equilibrium constant using the relationship $\Delta G = -RT \ln K$. By way of the expression $\Delta_r G = \Delta G_{\text{MoO}_3 \cdot 1.77\text{H}_2\text{O}(g)} - \Delta G_{\text{MoO}_3(g)} - \Delta G_{\text{H}_2\text{O}(g)}$, where $\Delta G_{\text{MoO}_3(g)}$ was taken from Pankratz (1982) and $\Delta G_{\text{H}_2\text{O}}$ was calculated using the program UNITHERM (Shvarov, 1991), the Gibbs free energy

for $MoO_3 \cdot 1.77H_2O$ was found to be 121.8792 kJ/mol. A water vapour pressure of 500 bars, which corresponds to a depth of roughly 5 km, if hydrostatic pressure is taken to be one third of the lithostatic load, was assumed for all calculations.

Molybdenite (MoS_2) is the primary ore mineral of Mo , and thus the solubility of Mo as $MoO_3 \cdot 1.77H_2O$ in the ore fluid (water vapour), which is significantly lower than that of Mo in a sulphur-free system (*i.e.*, experimental conditions), was calculated assuming equilibrium with molybdenite using the reaction:



The Gibbs free energy of reaction (3) was calculated using data from UNITHERM (Shvarov, 1991) and found to equal -189.689 kJ/mol. Fugacities of oxygen (fO_2) and sulphur (fS_2) were assumed to be those buffered by the assemblage hematite-magnetite-pyrite. Hematite and pyrite are commonly associated with MoS_2 mineralization in fracture fillings of Climax-type Mo -porphyry deposits, and magnetite is found in the magnetite-topaz alteration zone underlying the orebody (White *et al.*, 1981). Although the oxygen fugacity of the Mo -bearing ore fluid may in fact be slightly lower than the hematite-magnetite buffer, this reaction was chosen for simplicity. Gibbs free energies of the hematite-magnetite and magnetite-pyrite reactions were calculated using UNITHERM (Shvarov, 1991). At 600°C and 500 bars, $\log fO_2$ was found to be -14.74, and $\log fS_2$ to be -0.85. The fugacity of $MoO_3 \cdot 1.77H_2O$, which was calculated to equal -5.32, was then used to estimate the time required for the formation of a Mo -porphyry deposit via vapour transport.

Assuming that $\log f\text{MoO}_3 \cdot 1.77\text{H}_2\text{O}$ is the primary *Mo* species in the vapour phase, the logarithm of the mole fraction of *Mo* ($\log X_{\text{Mo}}$) in the system is equal to $\log f\text{MoO}_3 \cdot 1.77\text{H}_2\text{O}$ over $\log f\text{H}_2\text{O}$, and has a value of -7.91. This converts to a *Mo* solubility of 0.064 ppm. Using a water vapour flux of 5 million tonnes per year, as observed at the actively degassing Satsuma-Iwojima volcano, Japan (Saito *et al.*, 2001), 0.32 tonnes per year *Mo* is transported in the vapour phase. Assuming that all parameters outlined above remain constant and all *Mo* is deposited in a single location, the formation of an economic *Mo* orebody such as the Endako porphyry deposit, BC (336 Mt at 0.087% *Mo*) would take 906,601 years.

References

- Belton, G.R. and Jordan, A.S. (1965) The volatilization of molybdenum in the presence of water vapor. *J. Phys. Chem.* 69: 2065-2071.
- Pankratz, L.B. (1982) *Thermodynamic Properties of Elements and Oxides*. United States Bureau of Mines, Bulletin 672, 509 pp.
- Saito, G., Kazahaya, K., Shinohara, H., Stimac, J., and Kawanabe, Y. (2001) Variation of volatile concentration in a magma system of Satsuma-Iwojima volcano deduced from melt inclusion analyses. *J. Volcanol. Geotherm. Res.* 108: 11-31.
- Shvarov, Y. (1991) UNITHERM thermodynamics software, Department of Geology, Moscow State University.
- White, W.H., Bookstrom, A.A., Kamilli, R.J., Ganster, M.W., Smith, R.P., Ranta, D.E. and Steininger, R.C. (1981) Character and origin of Climax-type molybdenum deposits. *Econ. Geol.* 75th Anniversary Volume: 270-316.